Intraregional Comparisons of the Near-Storm Environments of Thunderstorms with Typical and Anomalous Charge Structure

Alexander J Eddy[1], Donald MacGorman[2], Cameron Homeyer[3], and Earle Williams[4]

[1]NOAA/NSSL/University of Oklahoma/CIMMS
[2]NOAA/National Severe Storms Lab
[3]University of Oklahoma/School of Meteorology
[4]Massachusetts Institute of Technology

November 24, 2022

Abstract

We gridded eleven years of cloud-to-ground (CG) flashes detected by the U.S. National Lightning Detection Network during the warm season in 15 km x 15 km x 15 min grid cells to identify storms with substantial CG flash rates clearly dominated by flashes lowering one polarity of charge to the ground or the other (+CG flashes versus –CG flashes). Previous studies in the central United States had found that the gross charge distribution of storms dominated by +CG flashes included a large upper negative charge over a large middle level positive charge, a reversal of the usual polarities. In each of seven regions spanning the contiguous United States (CONUS), we compared the values of 17 environmental parameters of storms dominated by +CG flashes with those of storms dominated by –CG flashes. These parameters were chosen based on their expected roles in modulating supercooled liquid water content (SLWC) in the updraft because laboratory experiments have shown that SLWC affects the polarity of charge exchanged during rebounding collisions between riming graupel and small ice particles in the mixed phase region. This, in turn, would affect the vertical polarity of a storm's charge distribution and the dominant polarity of CG flashes. Our results suggest that the combination of parameters conducive to dominant +CG flash activity and, by inference, to anomalous storm charge structure varies widely from region to region, the lack of any favorable parameter value in a given region being offset by favorable values of one or more other parameters.

Intraregional Comparisons of the Near-Storm Environments of Thunderstorms with Typical and Anomalous Charge Structure

A. J. Eddy[1,2*], D. R. MacGorman[1,2,3], C. R. Homeyer[2], and E. Williams[4]

[1] Cooperative Institute for Mesoscale Meteorological Studies, University of Oklahoma and NOAA/National Severe Storms Laboratory (NSSL), Norman, OK, USA.
[2] School of Meteorology, University of Oklahoma, Norman, OK, USA.
[3] NSSL, Norman, OK, USA.
[4] Massachusetts Institute of Technology, Cambridge, MA, USA.

*Corresponding author: Alexander Eddy (ajeddy@tx.rr.com)

Key Points:

- Storms dominated by frequent positive or negative ground flashes were mined from 11 years of National Lightning Detection Network data.
- The near-storm environments of storms dominated by frequent positive or negative ground flashes were compared in each of seven regions.
- The combination of environmental parameters inferred to have produced storms with anomalous charge structure varied from region to region.

Abstract

We gridded eleven years of cloud-to-ground (CG) flashes detected by the U.S. National Lightning Detection Network during the warm season in 15 km x 15 km x 15 min grid cells to identify storms with substantial CG flash rates clearly dominated by flashes lowering one polarity of charge to the ground or the other (+CG flashes versus –CG flashes). Previous studies in the central United States had found that the gross charge distribution of storms dominated by +CG flashes included a large upper negative charge over a large middle level positive charge, a reversal of the usual polarities. In each of seven regions spanning the contiguous United States (CONUS), we compared the values of 17 environmental parameters of storms dominated by +CG flashes with those of storms dominated by –CG flashes. These parameters were chosen based on their expected roles in modulating supercooled liquid water content (SLWC) in the updraft because laboratory experiments have shown that SLWC affects the polarity of charge exchanged during rebounding collisions between riming graupel and small ice particles in the mixed phase region. This, in turn, would affect the vertical polarity of a storm's charge distribution and the dominant polarity of CG flashes. Our results suggest that the combination of parameters conducive to dominant +CG flash activity and, by inference, to anomalous storm charge structure varies widely from region to region, the lack of any favorable parameter value in a given region being offset by favorable values of one or more other parameters.

Plain Language Summary

Thunderstorms with much greater amounts of small liquid droplets in updrafts at heights with temperatures less than 0°C have been found to have reversed the relative heights of positive and negative charge from what is normally observed. Lightning strikes to ground in these unusual storms tend to lower positive charge to ground instead of the usual negative charge. In this study, we analyzed eleven years of cloud-to-ground lightning flash data from the U.S. National Lightning Detection Network to identify individual storms in which very high or very low percentages of lightning ground strikes lowered positive charge to the ground. We then compared the environments of the two types of storms. Various combinations of environmental characteristics expected to enhance the amount of liquid droplets at temperatures less than 0°C were associated with storms having ground strikes dominated by flashes that lowered positive charge to ground, but the specific combination varied from one region to another. No environmental property that we evaluated appeared to be important in all regions. We infer, therefore, that the combination of environmental conditions that causes inverted-polarity thunderstorms also varies from region to region.

1. Introduction

Our goal for this study was to examine environmental conditions conducive to producing storm charge distributions with an inverted vertical polarity, with positive charge at middle levels of storms (roughly −10 to −20°C) where negative charge typically is observed and negative charge at upper levels of storms (roughly −40 to −50°C) where positive charge typically is observed. That warm-season storms could have such a charge distribution was first demonstrated definitively by the STEPS field program in northwestern Kansas, southwestern Nebraska, and northeastern Colorado in 2000 (Lang et al., 2004; Rust & MacGorman, 2002; Rust et al., 2005). A major goal of STEPS was to determine what storm characteristics were responsible for producing storms in which most cloud-to-ground (CG) flashes lower positive charge to ground instead of the usual negative charge, itself an unexpected observation made possible by the advent of networks for automatically mapping lightning ground strikes that lowered either polarity of charge to ground (e.g., Krider et al., 1980; MacGorman & Taylor, 1989; Orville, 2008): Although <10% of CG flashes in most regions of the CONUS lower positive charge to ground (+CG flashes), rather than the usual negative charge (−CG flashes; e.g., Orville & Huffines, 2001; Boccippio et al., 2001), most of the cloud-to-ground lightning produced by some warm-season storms are +CG flashes (Branick & Doswell, 1992; Curran & Rust, 1992; MacGorman & Burgess, 1994; Reap & MacGorman, 1989; Siemon, 1993; Smith et al., 2000). A definitive explanation for these anomalous storms was initially difficult to establish, however, because such storms are rare in most regions and establishing an explanation required in-storm soundings of the electric field with concurrent four-dimensional maps of in-cloud lightning, a combination unavailable in regions typically producing such storms until almost 2000. The STEPS region was selected for intensive study because it had an unusually large rate of +CG flashes (e.g., Boccippio et al., 2001; Lang et al., 2004; Orville & Huffines, 2001). What was found was that STEPS storms in which most CG flashes were +CG flashes all had inverted-polarity charge distributions (MacGorman et al., 2005; Rust et al., 2005; Tessendorf et al., 2007a, 2007b; Weiss et al., 2008; Wiens et al., 2005).

An obvious question then was: What environments produce storms with anomalous charge distributions? As described in the following section, studies of storms with anomalous charge distributions have offered a number of hypotheses for the environmental processes responsible for producing these storms, but these explanations have focused mainly on storms in the STEPS region or in Oklahoma and north Texas. All of these hypotheses have involved processes that enhance supercooled liquid water content because laboratory studies (e.g., Emersic & Saunders, 2010; Jayaratne et al., 1983; Saunders & Peck, 1998; Takahashi, 1978; Takahashi & Miyawaki, 2002) have found that unusually large concentrations of supercooled liquid water content (SLWC) cause graupel in the mixed-phase region to gain positive charge during rebounding collisions with smaller ice particles regardless of temperature.

Two of the previous studies that examined environmental influences on the polarity of charge distributions used data from the National Lightning Detection Network (NLDN, Orville, 2008; Cummins and Murphy, 2009) in Oklahoma, Kansas, and the Texas panhandle (Carey & Buffalo, 2007) or in the STEPS region (Lang & Rutledge, 2011) to identify storms in which +CG flashes constituted an unusually large fraction of their CG activity. Like them, the present study examines a broad range of environmental influences, but it broadens the scope of previous

studies by analyzing storms across the whole of CONUS. At a minimum, this is the first CONUS-wide climatological study of storms in which +CG flashes constitute a large percentage (≥80%) of frequent CG flashes detected by the NLDN. Our inference, supported by the studies mentioned above in the central United States, is that storms with large +CG percentage thresholds have inverted-polarity vertical charge structure. This inference needs to be verified eventually in other regions, as there is a lack of internal storm soundings with electric field measurements characteristic of inverted-polarity charge structure in storms outside of the central CONUS. The criteria we chose for including storms in our study were intended to focus on deep convective cells during the warm season and to eliminate or minimize the influence of other storm scenarios in which CG activity can be dominated by +CG flashes, such as winter storms and the stratiform region of mesoscale convective systems, which are influenced by different environmental parameters.

2. Hypothesized Processes Affecting the Polarity of Storm Charge Distributions

2.1. Microphysical Processes

As noted above, a highly simplified description of the charge distribution typical of the updraft region of storms is that it consists of a large positively charged region in the upper part of storms, a large negatively charged region at middle levels, and a smaller positive charge often at lower levels (roughly 0 to −10°C), with negative charge also along and near the upper cloud boundary (e.g., Brook et al., 1982; MacGorman & Rust, 1998; Simpson & Robinson, 1941; Stolzenburg et al., 1998; Takagi et al., 1986; Williams, 1989; Wilson, 1916, 1921). This simplified model is often called a dipolar or tripolar storm charge distribution model, depending on whether the lower positive charge is included. Outside of updrafts, charge distributions typically are more complex, with more vertically stacked charge regions (e.g., Bruning et al., 2014; Stolzenburg et al., 1998).

Laboratory results (e.g., Emersic & Saunders, 2010; Jayaratne et al., 1983; Jayaratne et al., 1984; Saunders & Peck, 1998; Saunders et al., 1991; Takahashi, 1978; Takahashi & Miyawaki, 2002) and numerical storm simulations (e.g., Helsdon et al., 2001; Mansell et al., 2005, 2010; Ziegler et al., 1991) suggest that the noninductive charging mechanism involving rebounding collisions between small ice particles and rimed graupel in the presence of supercooled liquid water content (SLWC) can explain the formation of the tripolar charge structure. They have noted that, at most temperatures and with moderate liquid water contents in the mixed-phase region of storms, graupel particles (smaller ice particles) gain negative (positive) charge during collisions, and that subsequent differential sedimentation in an updraft then produces the upper two charge regions. However, the polarity of the charge exchange is reversed at temperatures roughly ≥-10°C, and this accounts for the small lower positive region and contributes to the negative region. The existence of the lower positive charge region is important for the production of most –CG flashes (e.g., Clarence & Malan, 1957; Gilmore & Wicker, 2002; Jacobson & Krider, 1976; MacGorman et al., 2011; Mansell et al., 2002). When analyzing collisions between soft hail and ice crystals, Baker et al. (1987) found that the faster-growing particle tended to acquire positive charge.

As noted above, what appears to be important for producing an anomalous storm charge distribution is having sufficiently large values of SLWC because the laboratory studies (e.g., Saunders & Peck, 1998; Takahashi, 1978) have shown that sufficiently high values of SLWC

would cause graupel to charge positively during rebounding collisions throughout most or all of the depth of the mixed-phase region. Williams et al. (1991) found that graupel in such conditions would likely be undergoing wet growth, but there has been a paucity of in situ observations to confirm this. If graupel gains positive charge and small ice particles gain negative charge in an updraft, then after differential sedimentation the main charge regions would consist of an upper negative charge over a middle level positive charge, i.e., an inverted charge distribution. MacGorman et al. (2008, 2011) pointed out that within updrafts in which this was true, positive charge would be the lowest charge region throughout the depth of the charging process, so the small lower negative charge thought to be needed for +CG flashes (e.g., Rust et al., 2005, Tessendorf et al., 2007) would be absent. MacGorman et al. (2008, 2011) suggested that the lower negative charge might still be produced in adjoining regions in various ways, such as by precipitation in regions of weaker updraft or in adjoining cells that were settling as they dissipated.

2.2. Environmental Influences on Supercooled Liquid Water Content

The environmental parameters analyzed in our study, therefore, were suggested by previous studies as possibly influencing supercooled liquid water content enough to invert the polarity of a storm's vertical charge distribution:

Williams et al. (2005) suggested that the combination of high CAPE and high cloud base height (CBH) in the High Plains region played an important role in increasing SLWC to sufficiently high values. Higher CAPE would increase updraft speed, reducing the amount of time spent by an air parcel below the freezing level (hereafter called warm cloud residence time), where precipitation-sized raindrops scavenge cloud droplets through collision-coalescence and reduce their contribution to the SLWC in the mixed phase region. Higher CBHs would reduce the depth of warm cloud, again reducing the warm cloud residence time of hydrometeors and increasing the SLWC in the mixed phase region. Additionally, Williams et al. suggested a higher CBH would tend to cause broader updrafts, reducing entrainment in the updraft core and allowing more efficient processing of the CAPE and less dilution of SLWC there.

Carey and Buffalo (2007) analyzed environmental parameters taken from soundings in mesoscale regions with at most 25% +CG flashes and compared them to parameters in environments with higher +CG flash percentages. They found that the regions with higher percentages of +CG flashes (and therefore, potentially inverted-polarity storms) were associated with several environmental properties: a shallower warm cloud depth (WCD), a higher CBH, lower precipitable water (PWAT) from the surface to 400 hPa, a greater dew point depression (DPD), greater 0-3 km shear and storm-relative helicity (SRH), less convective inhibition (CIN), a lower equilibrium level (EL), smaller CAPE from the level of free convection (LFC) to -10°C, and greater normalized CAPE (NCAPE, the CAPE divided by the depth over which CAPE is realized) from the LFC to the EL. Other environmental parameters had similar values in the two populations of storms: CAPE from the LFC to the EL, NCAPE from the LFC to -10°C, equivalent potential temperature (θ_e), storm-relative wind speed at the EL, and 0-6 km shear. It seems counterintuitive that regions in which storms had larger +CG percentages were found to have a drier low-to-mid troposhere than the regions with lower +CG percentages, if the larger percentages were caused by storms having inverted-polarity charge structure, because larger

SLWCs are thought to be needed to produce inverted-polarity storms. In fact, Carey and Buffalo (2007) found that the adiabatic liquid water content (the maximum available water content that could be realized through adiabatic ascent) at the -20°C level in regions with larger +CG flash percentages was two-thirds that in regions with smaller +CG flash percentages.

To explain how there could then be a greater SLWC in the mixed-phase region, Carey and Buffalo (2007) proposed that, in regions of storms with larger +CG flash percentages, the higher CBH, shallower WCD, higher CAPE and NCAPE, and greater dynamical forcing of the updraft would increase the actual SLWC in the mixed-phase region by allowing enough of the actual liquid water content to survive into the mixed-phase region, as suggested by Williams et al. (2005), thereby more than compensating for the difference in adiabatic water content. They cautioned that no single environmental parameter could determine the polarity of a storm's charge distribution, but that a favorable combination could. They noted, for example, that even though WCD and CBH were among the most important parameters for the mesoscale regions they studied, high percentages of +CG flashes are seldom found in the desert southwest (where storms tend to have very high CBHs and shallow WCDs) perhaps due to insufficient CAPE.

Lang and Rutledge (2011) analyzed over 28,000 storm cells from the STEPS field program and compared cells with ≥50% +CG flashes to those having <50%. They found that the +CG-dominated cells had an inverted-polarity charge structure inferred from Lightning Mapping Array data and had almost twice the CAPE but slightly lower CBHs and slightly deeper WCDs. They did not consider this a refutation of the shallower WCD hypothesis for inverted-polarity storms but instead claimed that differences in CBH and WCD may be more important when comparing storms across different regions having different environmental characteristics than when comparing storms within a given region. They also found that +CG-dominated storms were associated with environments having greater SRH, higher storm heights, and greater 0-3 km and 0-6 km shear, which are environments that tend to produce greater dynamical forcing of the updraft

In a comparison of environmental conditions among locations with Lightning Mapping Arrays (the STEPS region, Oklahoma, Alabama, and the region around Washington, DC), Fuchs et al. (2015) found that storm cells with anomalous charge structure near the Oklahoma Lightning Mapping Array tended to have higher NCAPE than normal-polarity storms and those near the Colorado Lightning Mapping Array tended to have higher CBHs. They suggested that both environmental conditions could affect SLWC by controlling the warm cloud residence time, so one could therefore compensate for the other. Again, the finding of different combinations of environmental conditions in different regions being favorable for anomalous charge distributions could further explain both the similarities and differences among the findings by Carey and Buffalo (2007), Lang and Rutledge (2011), and their study.

A study of environments conducive to different classes of supercell storms focused on another environmental parameter which we would expect also to influence SLWC. Rasmussen and Straka (1998) analyzed the environments of low-precipitation (LP), classic (CL), and heavy-precipitation (HP) supercell storms. Unlike the other two supercell types, an LP supercell storm has little precipitation in or near its strong updraft, but has most of its precipitation and hail downstream in its anvil. Rasmussen and Straka found that LP storms have much stronger storm-

relative winds at anvil altitudes than HP storms have, with CL storms having intermediate values. Because it typically takes 10-30 min for precipitation to form in a supersaturated parcel (e.g., Young, 1993) and the residence time of a parcel in a supercell updraft core is around 10 min or less, they suggested that precipitation in a supercell updraft probably is caused by ingesting hydrometeors from outside the updraft, as well as by precipitation being grown in the fringes of the updraft. They suggested that the stronger anvil-level storm-relative wind of LP storms tends to transport hydrometeors well away from the updraft, thereby greatly reducing the concentrations ingested into the updraft and accounting for the relative lack of precipitation there.

Supercell storms in the region of the STEPS field program are initially most likely to be LP storms, so MacGorman et al. (2011) suggested that an environmental parameter favorable to LP storms could well also contribute to the greater tendency for storms in that region to have inverted-polarity charge structure. Having less precipitation in the inflow to updrafts would mean less competition for liquid water content below the mixed phase region and so would be more likely to produce inverted-polarity charge distributions. Thus, MacGorman et al. suggested that, in addition to WCB and CBH, the effect of strong anvil-level wind contributed to the greater tendency for storms in the region to have inverted-polarity charge distributions, and so caused their initial CGs often to be dominated by +CG flashes, as observed.

3. Data and Methods

All CG flash data from the years 2004-2014 were obtained from Vaisala's National Lightning Detection Network (NLDN) (Cummins & Murphy, 2009). We chose this analysis period in order to ensure consistent network specifications as it spanned the period between two major upgrades to the NLDN, one from 2002-2003 (Cummins & Murphy, 2009) and one in August 2015 (Nag et al., 2016). All flashes were gridded onto a 15 km x 15 km x 15 minute Cartesian grid spanning the CONUS using a Lambert Conformal conic projection (Snyder, 1987) The standard parallels chosen for the projection were 33°N and 45°N in order to minimize areal distortion across the CONUS (Alpha & Snyder, 1982). The grid was centered about a reference longitude of -95.8°E since this was the average of the westernmost and easternmost longitudes of our analysis domain. The analysis domain is shown in Figure 1.

We chose to grid only those +CG and –CG flashes with peak current magnitudes ≥15 kA, intending to remove most misclassified cloud pulses while not discarding too many real CG flashes, as would occur if we had chosen a higher threshold. Testing by the University of Arizona after the 2002-2003 upgrade showed that close to 90% of events with peak currents less than 10 kA that were interpreted as +CG flashes were actually misidentified cloud pulses (Cummins & Murphy, 2009). A similar situation was found for intracloud flashes (ICs) misidentified as –CG flashes in inverted-polarity storms (Calhoun et al., 2013; Fleenor et al., 2009). Because we intended to focus on inverted- polarity storms, we adopted the 15 kA threshold for both polarities of CGs.

Another possibility of contamination of +CGs in NDLN data has been raised by a recent study which found that the NLDN misclassified some compact intracloud discharges (CIDs) in Florida as large peak current +CGs (Leal et al., 2019). However, the reverse relationship, the fraction of NLDN-detected +CGs that are actually CIDs, may well be small, and previous studies suggest

this is the case. A study evaluating an older generation of NLDN technology in Oklahoma (MacGorman and Taylor, 1989) found that >90% of +CG flashes and –CG flashes with peak currents greater than approximately 15 kA had ELF signatures verifying they were CG flashes. The percentage was slightly lower for peak currents >35 kA, but was still approximately 90% for –CGs and only a couple of percentage points lower for +CGs. In a video study of +CGs detected in normal-polarity storms by the same version of the NLDN as used in this study, Biagi et al. (2007) found that the percentage of +CG strokes with peak currents >20 kA that had a verified channel to ground ranged from 67% to 95% in the storms they observed in north Texas and southern Oklahoma. Fleenor et al. (2009) analyzed +CGs detected mostly from inverted polarity storms in the CC region, again by the same NLDN version. Using video recordings and broadband electric field waveforms from the Los Alamos Sferic Array (LASA, Shao et al., 2006), they found that only one out of more than 1000 +CG strokes detected by the NLDN with a peak current >20 kA was actually due to an intracloud process.

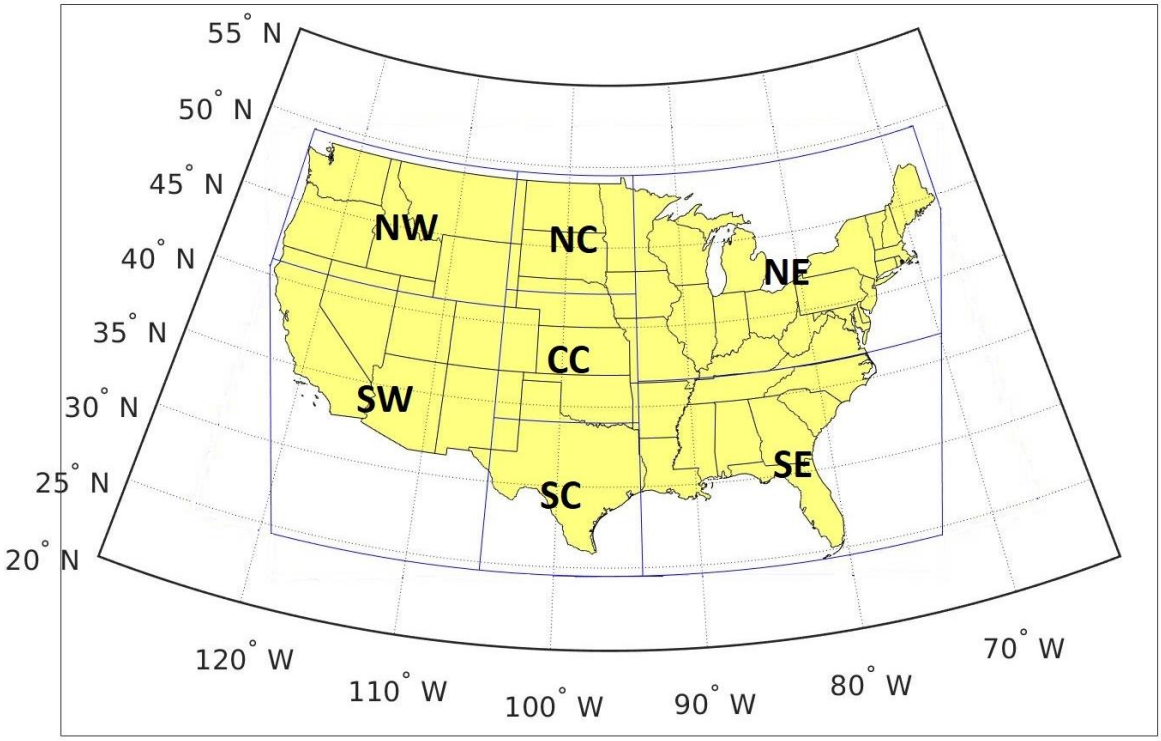

Figure 1. Boundaries of the analysis domain and the regions for evaluating environmental parameters favorable for +CGs. The analysis domain is bounded in blue. The CONUS and surrounding regions are divided into seven regions whose boundaries are also shown in blue: southwest (SW), northwest (NW), southcentral (SC), central-central (CC), northcentral (NC), southeast (SE), and northeast (NE).

Grid cubes were constructed every 5 km in the x- and y-directions and every 5 minutes in time. For our analysis, however, we chose grid cell dimensions of 15 km x 15 km by 15 minutes based on the typical spatiotemporal characteristics of an individual storm cell and constructed these larger grid cells by stepping forward every 5 km in x and y and every 5 min in time in order to determine the time and location of local maxima in flash counts with higher resolution, Grid cells were included in the analysis only if they had ≥10 CG flashes, ≥80% of which were +CGs, or if

they had ≥20 CG flashes, ≥90% of which were –CGs. The cells in the former (latter) group were inferred to be associated with inverted- (normal-) polarity electrical charge structure in the corresponding storm cell.

Because the intended focus of this study is on deep convective storm cells having inverted-polarity vertical charge structure, we attempted to minimize the influence of +CG flashes that can dominate CGs in many winter storms (e.g., Orville et al., 1987; Rudlosky & Fuelberg, 2011; Takeuti et al., 1978) or in the stratiform region of many mesoscale convective systems (e.g., MacGorman & Morgenstern, 1998; Makowski et al., 2013; Rutledge & MacGorman, 1988; Rutledge et al., 1993; Williams et al., 2010) by restricting our analysis in three ways: (1) We included data only from the warm season (defined below based on the region of the CONUS in which the cell was located). (2) Because MCSs tend to grow upscale from earlier convective storms and stratiform regions tend to peak starting around midnight (Maddox et al., 1986), we included only grid cells that occurred between 1500 and 2300 local time to attempt to minimize the impact of +CG-dominated grid cells from stratiform regions. (3) Because flash rates in a 15 km x 15 km stratiform region of an MCS are typically small, we chose a substantial total CG flash rate threshold of 10 (20) per 15 min in the case of the +CG- (–CG-) dominated cells.

Once the +CG- and –CG-dominated cells had been identified and the above filtering had been applied, the spatial and temporal overlap among grid cells was removed in order to reduce the amount of sample interdependence. This was carried out by ordering all grid cells from greatest number to least number of CG flashes and by working down the list cell by cell to eliminate cells that occurred within 15 km in space on all sides and within 30 minutes in time of the cell being considered (these thresholds may have eliminated some storm cells that were actually separate).

Once the dataset of +CG- and –CG-dominated cells had been built, environmental data from the North American Regional Reanalysis (NARR) dataset (Mesinger et al., 2006; NCAR/UCAR, 2019) was linked to each cell. Seventeen environmental parameters were analyzed, which we divided into three categories: moisture parameters, dynamic parameters, and thermodynamic parameters as follows:

- *Moisture parameters*
  Dewpoint depression at 2 m AGL (DPD), cloud base height (CBH), warm-cloud depth (WCD), and precipitable water (PWAT)
- *Thermodynamic parameters*
  Surface equivalent potential temperature (θ_e), convective available potential energy (CAPE) from the level of free convection (LFC) to the equilibrium level (EL), normalized CAPE from LFC to EL (NCAPE, i.e., CAPE divided by the distance between these two levels), LFC to -20°C CAPE, LFC to -20°C NCAPE, 0°C to -20°C CAPE, 0°C to -20°C NCAPE, convective inhibition (CIN), and EL altitude.
- *Dynamic parameters*
  0-3 km shear, 0-6 km shear, 0-3 km storm-relative helicity (SRH), and storm-relative wind speed at the EL.

It should be noted that the NARR does not directly assimilate surface temperature or dew point temperature. However, it does assimilate radiosonde data aloft and close to the surface. The NARR dataset provides data on 45 vertical levels on a 32 km x 32 km x 3 hour grid. Due to its

coarse resolution, we linearly interpolated in time and used the closest possible NARR grid point in space to obtain the values of each environmental parameter as close as possible to the time and location of each storm cell. Sometimes the characteristics of the environment interpolated from the NARR did not match characteristics that would be required to produce a cell with vigorous electrical activity. For example, some cells occurred at NARR grid points with 0 J kg^{-1} of CAPE from the LFC to EL. This could have also been the result of the storm itself affecting its nearby environment. To preserve only those cases in which the environment seemed less affected by nearby storm cells or in which interpolation did not lead to counterintuitive values, only those cells with an EL of at least 7 km were kept.

The CONUS was partitioned into seven regions: the southwest (SW), northwest (NW), southcentral (SC), central-central (CC), northcentral (NC), southeast (SE), and northeast (NE) regions (Figure 1); and the environmental parameters of +CG-dominated cells were compared with those of –CG-dominated cells within each region. The warm season was defined to be April-October in the SW, SC, and SE regions and from May-September in the other regions. This is the first study to compare the environmental differences favoring +CG production between these two categories of CG cells within each of several regions spanning the entire CONUS. Additionally, no other study has used +CG threshold percentages this high for +CG dominated cells and +CG threshold percentages this low for –CG dominated cells to distinguish cells with many +CG flashes from cells with few +CG flashes. Besides giving a climatology of +CG-dominated cells, we expect that the more extreme threshold percentages that we use here will better elucidate those environmental characteristics favorable for producing cells with anomalous charge structures. The sample sizes of +CG- and –CG-dominated cells for every region and environmental parameter are shown in Table 1. Overall, approximately 7.5% of the cells analyzed in the study were +CG-dominated.

For each region and for every environmental parameter, we determined the distribution of the values of the parameter for +CG-dominated cells and for –CG-dominated cells. Note that variations in climatological conditions within the individual regions probably affected our distributions, but regions needed to be fairly large to provide enough samples for our statistical analysis. We then conducted a permutation test (Wilks, 2011) to analyze whether the difference in median values for the two distributions was statistically significant. The test was two-tailed because we did not know a priori whether the median value of the parameter for the +CG-dominated cells would be greater or less than that for the –CG-dominated cells. The null hypothesis was that the two medians were not truly different in that region. For a given region and parameter, the test was carried out by taking the full sample set of the smaller of the two samples (usually the +CG-dominated cells), and an equal number of samples of the larger sample set chosen at random. After combining these two groups into one group, half of the group was chosen at random, and the median value of the parameter for that group and the median value for the remaining group were both calculated. The difference in these two median values was then calculated to give the value for one trial. The above steps were repeated for different randomly chosen groups for a total of 10,000 iterations, from which a null distribution of differences in the medians was generated. Then, the actual difference in medians of the two original unreduced samples was compared with the null distribution to calculate the significance level of the difference. Because the test was two-tailed, i.e., the actual median could be either less than or greater than median in the null distribution, the significance level S given as a percentage is: $\mathbf{S} = (\mathbf{100} - \mathbf{2n})\%$, where n is the smaller of either (1) the percentage of median differences in the

null distribution greater than the actual difference or (2) the percentage of median differences in the null distribution less than the actual median. The p-value is therefore bounded by $\boldsymbol{p < 1 - S}$. Differences in median were considered significant only if they were significant at the 90% level or higher.

Table 1
Sample sizes for each parameter & each region for the +CG- (–CG-) dominated cells with at least 10 (20) flashes & at least (at most) 80% (10%) +CG flashes. Percentage of +CG-dominated cells is also shown.

	SW	NW	SC	CC	NC	SE	NE
WCD and CBH	1494 (39891) 3.6%	528 (5112) 9.4%	1321 (58380) 2.2%	14006 (45909) 23.4%	11170 (7874) 58.7%	1148 (205020) 0.56%	4287 (116150) 3.6%
All other parameters	1581 (41472) 3.7%	639 (6254) 9.3%	1644 (62023) 2.6%	16640 (50098) 24.9%	13580 (9473) 58.9%	1207 (207640) 0.58%	4812 (119460) 3.9%

Note: The bottom parameter is the percentage of storm cells analyzed in each region that were +CG-dominated cells.

4. Geographic Distribution of –CG and +CG-Dominated Cells

Figure 2a shows the geographic distribution of –CG-dominated cells (≥20 flashes in 15 minutes, ≥90% being –CG flashes) across the CONUS. Much as for climatologies of –CG flashes and of total CG flashes (e.g., Medici et al., 2017; Orville & Huffines, 2001), there is an overall increase in the number of storm cells roughly from the NW to the SE, with the highest concentrations located in central Florida. This similarity is expected because roughly 90% of CG flashes in the CONUS are –CG flashes (Cooray, 2015). Figure 2b shows the distribution of +CG-dominated cells (≥10 flashes in 15 minutes, ≥80% being +CG flashes) across the CONUS. These cells are most commonly located in the High Plains region, which is also where inverted-polarity cells have been observed most frequently in studies (e.g., Fuchs et al., 2015; Lang & Rutledge, 2011; MacGorman et al., 2005; Rust & MacGorman, 2002; Rust et al., 2005; Tessendorf et al., 2007a, 2007b; Weiss et al., 2008; Wiens et al., 2005). Additionally, the local maxima in eastern Louisiana/southern Mississippi, southern Florida (also noted there by Marchand et al., 2019), eastern North Carolina, and in northwestern Mexico indicate the possible presence of inverted-polarity storm cells in those regions, although this has not yet been verified by independent storm-scale observations. Note that the larger +CG cell counts in Kansas, Nebraska, and the Dakotas correspond approximately to a trough of relative minima in –CG cell counts.

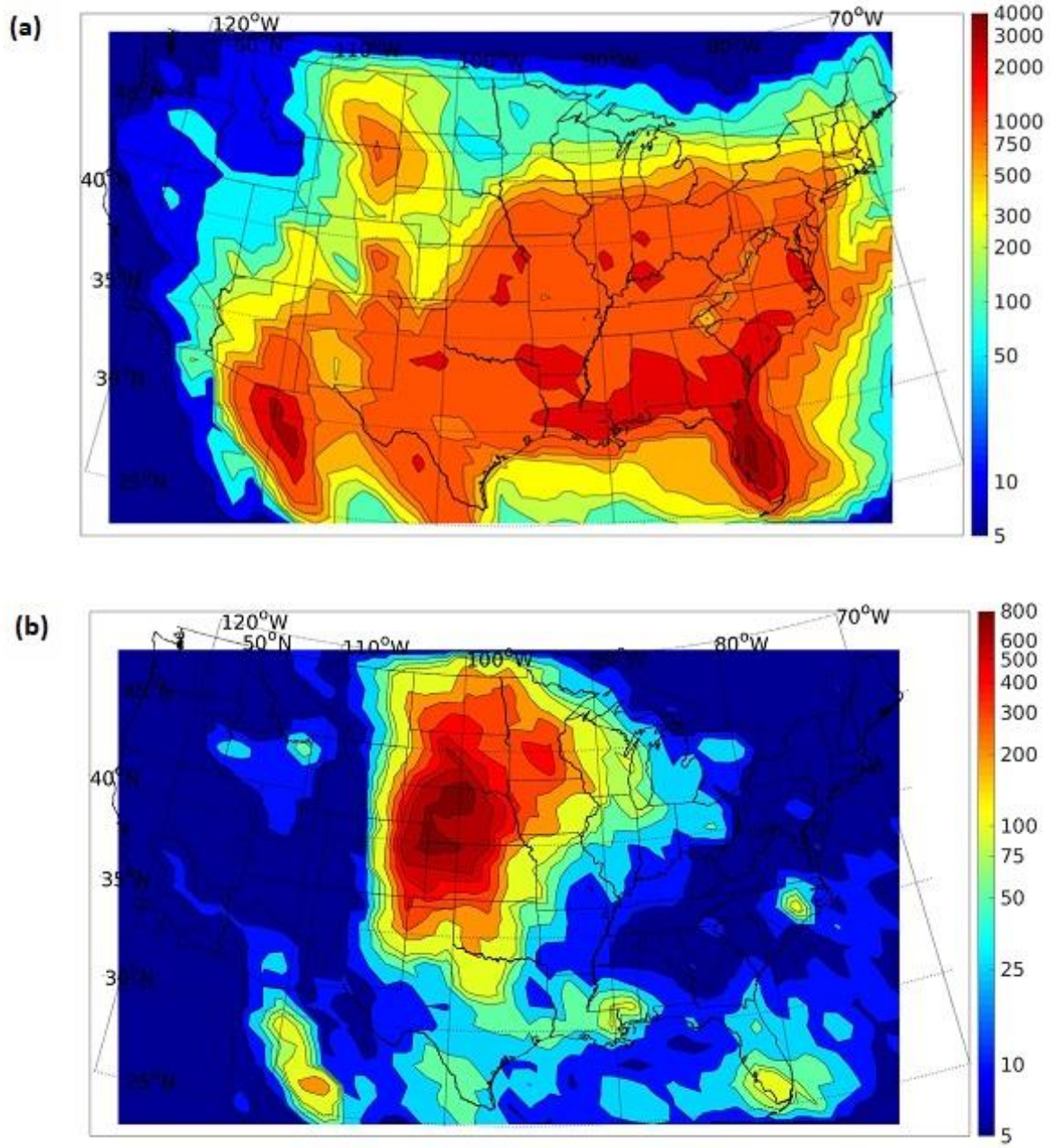

Figure 2. Number per 15 km x 15 km area of (a) –CG dominated cells, inferred to have normal-polarity charge structure and (b) +CG dominated cells, inferred to have inverted-polarity charge structure from 11 years of warm-season NLDN data, after the filtering described in Section 3. Note that the colorscale used is logarithmic, and each contour is labeled on the color bar.

5. Differences in the Environments of +CG-Dominated and –CG-Dominated Cells

The sections below show differences in median values of four moisture parameters: CBH, WCD, DPD, and PWAT (Figure 3); three thermodynamic parameters: LFC to EL CAPE, LFC to –20 °C CAPE, and CIN (Figure 4); and three dynamic parameters: 0-6 km shear, storm-relative wind speed at the EL, and SRH (Figure 5), between the two types of cells in each of the seven regions spanning the CONUS. Special emphasis will be placed in our discussion on the CC and NC regions because these two regions have a greater sample size of +CG-dominated cells than all of the other regions combined (Table 1). Furthermore, environmental controls on storm polarity have previously been studied more in the CC region than in any other region.

The distribution of values for each of these parameters is shown by violin plots for the two types of cells for each region. The width of the violin shape at a given value of a parameter is proportional to the number of storm cells having that value, normalized so that all violin plots have the same total area. The distributions for +CG (–CG) dominated cells are colored in red (blue). Black box-and-whisker plots are overlaid on the violins. The bottom of the black box indicates the 25^{th} percentile, the white circle within the black box indicates the median value of the distribution, and the top of the black box indicates the 75^{th} percentile. The percent difference in medians for the parameter in each region is also shown below the violin plots; a positive percent difference indicates that the median value for the +CG-dominated cells was greater. The p-value for the difference in median values is given below the corresponding percent difference of median values. P-values were determined from a two-tailed permutation test, described in Section 3. Each p-value can be multiplied by a factor of 100 to yield the probability (in percent) of achieving the given percent difference in median if there were truly no difference in the two populations of cells. Thus, a low p-value indicates that the median values of the parameter for +CG- and –CG-dominated cells are likely different, with a significance level $S = 100*(1 - p)$.

5.1. Moisture Parameters

5.1.1. Cloud Base Height

Williams et al. (2005) and Fuchs et al. (2015) suggested that higher CBHs increase SLWC in the updraft by decreasing the WCD (and therefore the warm cloud residence time). They also indicated that storms with higher CBHs tend to have broader, stronger updrafts, so the water content would be less diluted by dry-air entrainment in their updraft core and more water content would be transported to the mixed-phase region in the core. Figure 3(a) shows the distribution of CBHs for +CG-dominated cells and for –CG-dominated cells. All regions had significant differences in median CBHs, with $p < 0.0002$ (i.e., were significant at the 99.98% level).

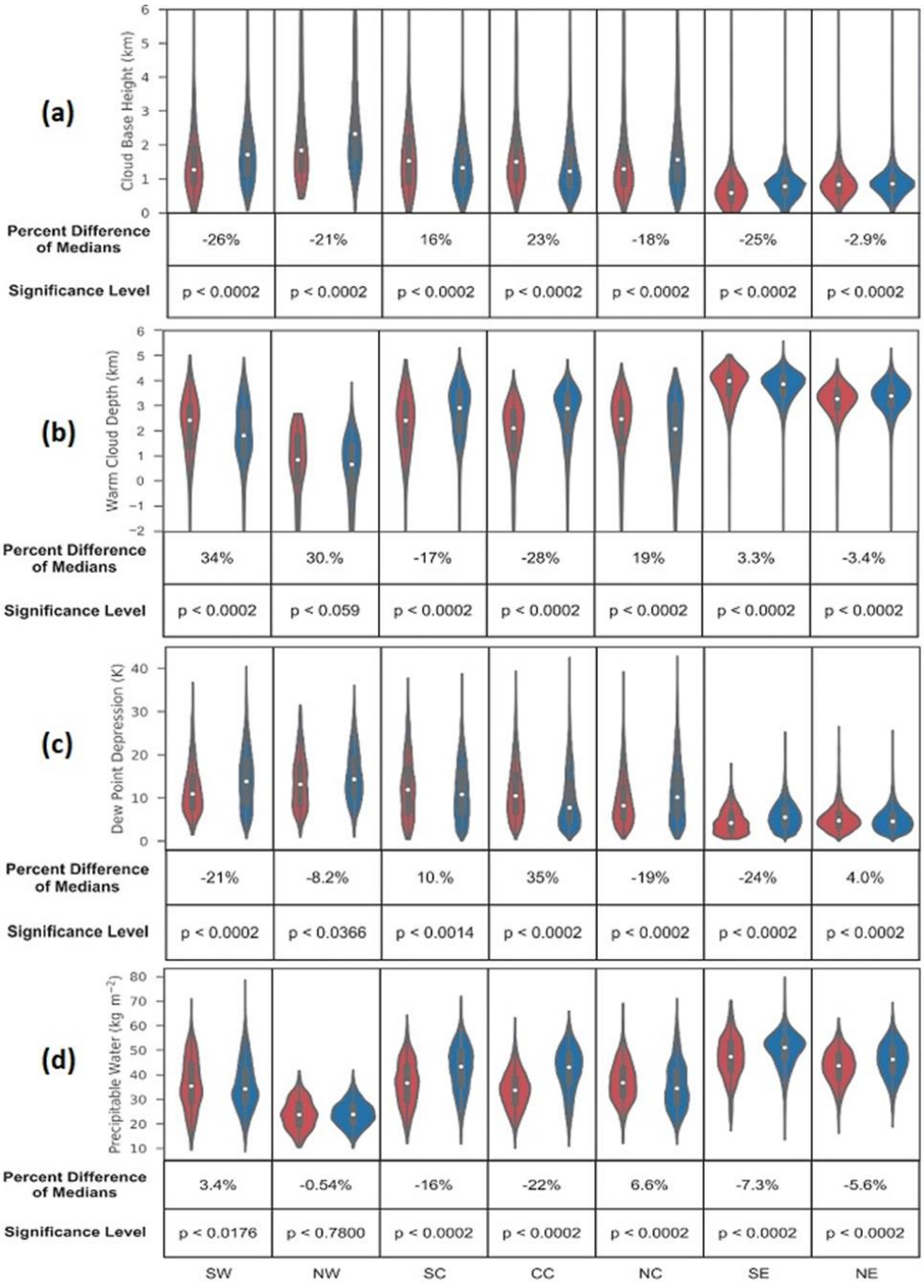

Figure 3. Violin plots of the moisture variables: (a) cloud base height, (b) warm cloud depth, (c) dew point depression, and (d) precipitable water for each region. Each violin plot is scaled such that all violins for a given variable have the same area, and the number of cells with a particular value of the given parameter is proportional to the width of the violin at that value. Red (blue) violins correspond to the +CG- (–CG-) dominated cells. See text for explanation of other aspects of the figure.

The SC and CC regions were the only regions with higher median CBHs in +CG-dominated storms than in –CG-dominated storms. In all other regions, median values of CBH were higher for –CG-dominated cells. The region containing cells with the highest median CBH for +CG-dominated cells was the NW region, but this region had the smallest sample size of +CG-dominated cells, and its median CBH for –CG-dominated cells was even higher. It seems contrary to the expectations of Williams et al. (2005) that the hypothesized relationship with CBH did not hold in the NC region, which had the second-highest sample size of +CG-dominated cells, although we shall see that their suggested role of superlative updrafts will be supported by other parameters analyzed in this paper. The fact that the median CBH was higher for −CG-dominated storm cells in all regions except the NC and CC regions suggests that the hypothesized role of CBH is not the only factor that can cause a cell's CGs to be dominated by +CGs, although it appears to have contributed in the SC and CC regions.

5.1.2. Warm Cloud Depth

A shallower WCD is a candidate for allowing higher SLWCs by decreasing the warm cloud residence time of parcels ascending in the updraft (e.g., Carey & Buffalo, 2007; Fuchs et al., 2015; Williams et al., 2005). Figure 3(b) shows the distribution of WCD in –CG- and +CG-dominated cells for all regions. In all regions except for the NW region, the difference in median WCD was significant at the 99.98% level, and it was significant at the 94.1% level in the NW region. A negative value of WCD meant that the cloud base was above the freezing level.

+CG-dominated cells in the CC region were found to have a median WCD that was 28% shallower than the region's –CG-dominated cells, but in the NC region +CG-dominated cells had a median WCD that was 19% deeper than –CG-dominated cells. The regions in which +CG-dominated cells had shallower WCDs were the SC, CC, and NE regions although the percent difference in the NE was very small.

In the remaining regions, median WCD was greater for +CG-dominated cells than for −CG dominated storms, although the percent difference was small in the SE. The NW region, which had the shallowest median WCD for +CG-dominated storms compared to any other region, had an even shallower median WCD for –CG-dominated storms. The fact that the median WCD for +CG-dominated storms was greater than the median for –CG-dominated storms in a majority of regions suggests that WCD is not by itself a sufficient factor for determining the polarity of a storm's charge distributions and the dominant polarity of its CGs.

5.1.3. Dew Point Depression

Several early studies found that supercell storms dominated by +CG flashes tended to occur in drier subcloud regions with larger DPDs (Knapp, 1994; MacGorman & Burgess, 1994; Smith et al., 2000), so our environmental analysis of DPD was intended to test whether this was generally true. Furthermore, DPD and CBH can be approximated to scale linearly with one another (Williams et al., 2005), so we would expect higher DPDs to favor greater SLWCs in a way similar to the influence hypothesized for CBH. Figure 3(c) shows the characteristics DPD in the environments of –CG- and +CG-dominated cells for all regions. The difference between the

median DPD of +CG-dominated cells and that of –CG-dominated cells was significant at ≥ 96.34% in all regions.

As one might expect, the regions in which the median difference in DPD was positive and, therefore, was hypothesized to favor +CGs, were the same as those in which WCD also was consistent with the +CG hypothesis: Only the CC, SC, and NE regions each had a positive percent difference in medians, although the difference was small in the NE. At 35%, the CC region had the largest difference in median DPDs favoring +CG-dominated cells. However, as with the trend for CBHs and WCDs, the DPDs in the SE, NC, SW, and NW regions actually had negative differences in median DPDs, which meant that –CG-dominated cells had larger median DBDs than +CG-dominated cells had and, therefore, would have been hypothesized to tend toward having less SLWC in the +CG dominated cells, a fact which argues against larger DPD being sufficient alone for producing +CG-dominated storms.

5.1.4. Precipitable Water

As for the other moisture parameters, we analyzed PWAT because Carey & Buffalo (2007) suggested that lower PWAT maximizes SLWC by reducing water loading in the updraft, which would suppress the collision-coalescence processes that act to deplete the smaller cloud droplets that contribute to the SLWC and reduce the entrainment of dry air, allowing more liquid water to ascend into the mixed-phase region. Furthermore, reduced water loading in the updraft could allow for stronger updrafts for the same amount of CAPE. The resulting reduced transit times for depleting SLWC below the mixed-phase region would allow a larger fraction of the liquid water to ascend into the mixed-phase region. If a lower PWAT has this effect, we would expect a tendency for +CG-dominated cells to have lower PWAT. Figure 3(d) shows the distribution of PWAT in –CG- and +CG-dominated cells for all regions.

Overall, the magnitudes of the percent differences in the median PWATs between +CG-dominated cells and –CG-dominated cells tended to be smaller than for the other moisture parameters. However, the differences in the medians were still significantly different at a level ≥ 98% in all regions except in the NW region, where the medians were not significantly different.

As for all the other moisture parameters, the CC and SC regions again displayed the largest magnitude of median percent differences favoring +CG-dominated cells according to the hypothesized process. The distributions of PWAT differed from the other moisture parameters in that the SE and NE regions also had a difference in median values of PWAT that was hypothesized to be more favorable for +CG-dominated cells. However, the SW and NC regions both had a difference in median values deemed unfavorable for producing +CG-dominated cells for all of the moisture variables, and the NC region had the second largest number of +CG-dominated cells. Thus, while PWAT may contribute to producing +CG-dominated cells (presumably having inverted-polarity charge distributions) in some regions, the fact that there were exceptions suggests that PWAT, like the other moisture variables, is not sufficient alone; other types of environmental parameters (i.e., thermodynamic or dynamic) must have favorable values in at least some situations.

5.2. Thermodynamic Parameters

5.2.1. LFC to EL CAPE

The hypothesis being tested here is that, even if warm cloud depths were larger than optimal values, greater updraft speeds would reduce the warm cloud residence time needed for precipitation growth in an ascending air parcel and so might enhance the amount of SLWC enough to produce an inverted-polarity charge distribution (e.g., Fuchs et al., 2015, 2018; Williams et al., 2005). Figure 4(a) shows the distribution of LFC to EL CAPE in –CG- and +CG-dominated cells for all regions. The difference in median values was statistically significant at the 98.98% level in all regions except in the NW region, where it was significant at the 92.84% level, and in the SE region, where it was not statistically significant.

In all regions except the CC region, +CG-dominated cells had larger median values of CAPE than –CG-dominated cells had. The largest favorable percent differences by far were for the SW and NC regions, where differences in median values for moisture parameters uniformly favored –CG-dominated cells rather than +CG-dominated cells. Thus, the additional LFC to EL CAPE needed to produce +CG-dominated storms appeared to be especially great in the SW and NC regions. The difference in medians for the CC region was not large, but favored –CG-dominated cells, while the differences for all the moisture parameters favored +CG-dominated cells there. It appears, therefore, that favorable values of CAPE through the depth of the storm tended to overcome unfavorable values of the moisture parameters. The environment of cells in the NW region had the lowest median LFC to EL CAPE, and this may help explain why the NW region had the fewest observations of cells dominated by either polarity of CGs.

5.2.2. CAPE from the LFC to -20°C

CAPE through the layer from the LFC to -20°C considers the effect of updraft speed in the middle of the mixed-phase region rather than considering the whole depth of the storm. Figure 4(b) shows the distributions of LFC to -20°C CAPE in –CG- and +CG-dominated cells for all regions. As in the case of LFC to EL CAPE, all the medians were statistically different at the 99.98% level except in the NW region, where the difference in median was statistically significant at the 98.78% level, and in the SE region, where the median difference was not statistically different.

Once again, it appears clear that no one environmental parameter clearly leads to +CG-dominated or –CG-dominated cells (and by inference, to inverted- or normal-polarity cells). The median LFC to -20°C CAPE was larger for +CG-dominated cells in all regions with statistically significant differences except in the CC region. In the CC region, the median LFC to -20°C CAPE for +CG-dominated cells was 17% smaller than that for –CG-dominated cells; although LFC to -20°C CAPE was unfavorable, all the moisture parameters considered in previous sections tended to be favorable. On the other hand, as for LFC to EL CAPE, the percent difference in median LFC to -20°C CAPE was largest by far for the NC and SW regions, so this parameter was a good discriminator between the two categories of cells there, although the median moisture parameters in those regions tended to be unfavorable for +CG-dominated cells.

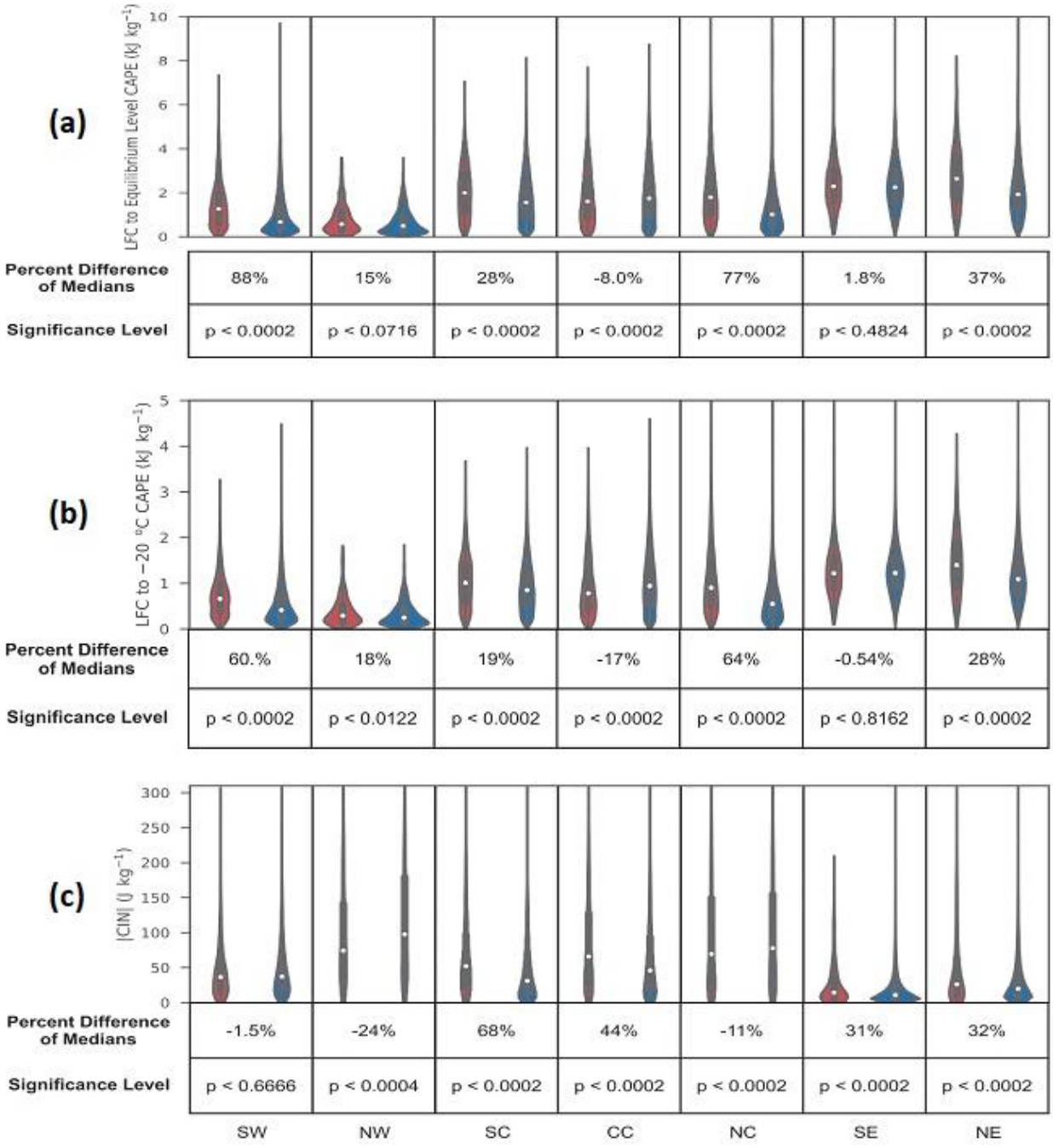

Figure 4. Violin plots of the thermodynamic variables: (a) LFC to EL CAPE, (b) LFC to −20°C CAPE, and (c) |CIN| for each region. Red (blue) violins correspond to the +CG- (–CG-) dominated cells. See text and caption for Figure 3 for more explanation of the figure.

Note also that the magnitude of the median LFC to -20°C CAPE for +CG-dominated cells was not as important as its value relative to the median for –CG-dominated cells. One of the largest median values for +CG-dominated cells occurred in the SE region, yet the difference in the medians for the two categories of CGs in that region was not significantly different.

5.2.3. CIN

We analyzed the magnitude of CIN because, all else being equal, shifting the temperature at which a parcel attains free convection to higher temperatures tends to make the storms that do occur more isolated, with less competition for inflowing air and moisture, and thereby to increase the CAPE realized by parcels above the LFC. Thus, storms that do form with larger magnitudes of |CIN| tend to be stronger storms (Fuchs et al., 2018; Rasmussen & Houze, 2016), with stronger updrafts, resulting in shorter warm-cloud residence times and greater supersaturation in the mixed phase region. We hypothesize, therefore, that environments with greater |CIN| are more conducive to realizing greater SLWCs. Figure 4(c) shows the distributions of |CIN| in –CG- and +CG-dominated cells for all regions. The median values of |CIN| for +CG-dominated and –CG-dominated cells were significantly different in all regions at the 99.96% level or higher except in the SW region, where they were not significantly different.

In the SC and CC regions, |CIN| was the parameter with the largest percent difference supporting the hypothesis regarding +CG-dominated cells. It also supported the hypothesis in the SE and NE regions, but not in the NW, NC, and SW regions. The failure of the hypothesis in some regions, particularly in the NC region which had the second largest number of +CG-dominated cells, again means that this parameter cannot solely account for +CG domination. Furthermore, the largest median magnitude of |CIN| was for –CG-dominated cells in the NW, not for +CG-dominated cells there, so again, the absolute median value of |CIN| was not as important as the difference in median values between the two categories of storm cells.

5.3 Dynamic Parameters

5.3.1. 0–6 km Shear

Because stronger 0-6 km shear is more conducive to rotating updrafts, and updraft rotation causes dynamic pressure gradient forces that can strengthen the updraft (Weisman & Klemp, 1982, 1984), we hypothesized that environments supporting greater 0-6 km shear would support storms with stronger updrafts and therefore shorter warm cloud residence times. Thus, environments with greater 0-6 km shear may tend to have greater SLWCs in the mixed-phase region.

Figure 5(a) shows the distributions of 0-6 km shear in environments containing –CG- and +CG-dominated cells for all regions. The difference in medians was not statistically significant in the NW region. In all other regions, the difference in median values of 0-6 km shear favored higher SLWCs in +CG-dominated cells than in –CG-dominated cells. The percent difference in median 0-6 km shear in each of the three southern regions was larger than the percent difference in each adjoining region north of it, with the two largest magnitudes of percent difference being in the SE and SC regions. Note that having a large value of 0-6 km shear was not sufficient in itself to

satisfy our hypothesis, as the NW region had relatively large median values, but the difference in medians was not significantly different.

5.3.2. Storm-Relative Wind Speed at the Equilibrium Level

We calculated storm-relative wind speed at the EL by subtracting the non-pressure-weighted mean of the wind from 0-6 km from the wind at the EL. We chose to analyze this parameter because MacGorman et al. (2011, 2017) hypothesized that storms with stronger such quantity at the EL would loft more of the precipitation too far downstream from near the top of an updraft for it to be recirculated back into the updraft. Williams et al. (2005) had noted that the region with more +CG flashes and anomalous charge distributions also tended to have more low-precipitation storms, and the effect of strong anvil-level winds had been noted by Rasmussen and Straka (1998) to explain why some supercell environments produced low-precipitation supercell thunderstorms. Fewer precipitation-sized particles in the updraft below the freezing level would lead to higher concentrations of small cloud droplets and larger values of SLWC in the mixed-phase region because fewer precipitation-sized particles would be available to scavenge cloud droplets through warm-cloud collision-coalescence processes.

Figure 5(b) shows the distribution of storm-relative wind speed at the EL in environments containing either +CG-dominated or –CG-dominated cells for all regions. The difference in median values was significant at a level >93% in all regions and the median was greater for +CG-dominated cells in all regions except in the NW region. The difference in median values was greatest by far in the SC region, followed by the two eastern regions. The fact that the median storm-relative wind speed at the EL in the NW region was greater for –CG-dominated storms and was relatively small in two other regions suggests that it is not the only important environmental parameter for producing +CG-dominated storms, although it appears to play a role in at least some regions.

5.3.3. 0-3 km Storm-Relative Helicity

We chose to analyze SRH because greater SRH provides greater dynamical forcing of the updraft (Carey & Buffalo, 2007; Weisman & Klemp, 1982) by causing it to rotate, potentially increasing updraft speed due to the dynamic pressure perturbations associated with rotation. Stronger updrafts allow shorter warm cloud residence times, which increases SLWC as described in Section 2.2.

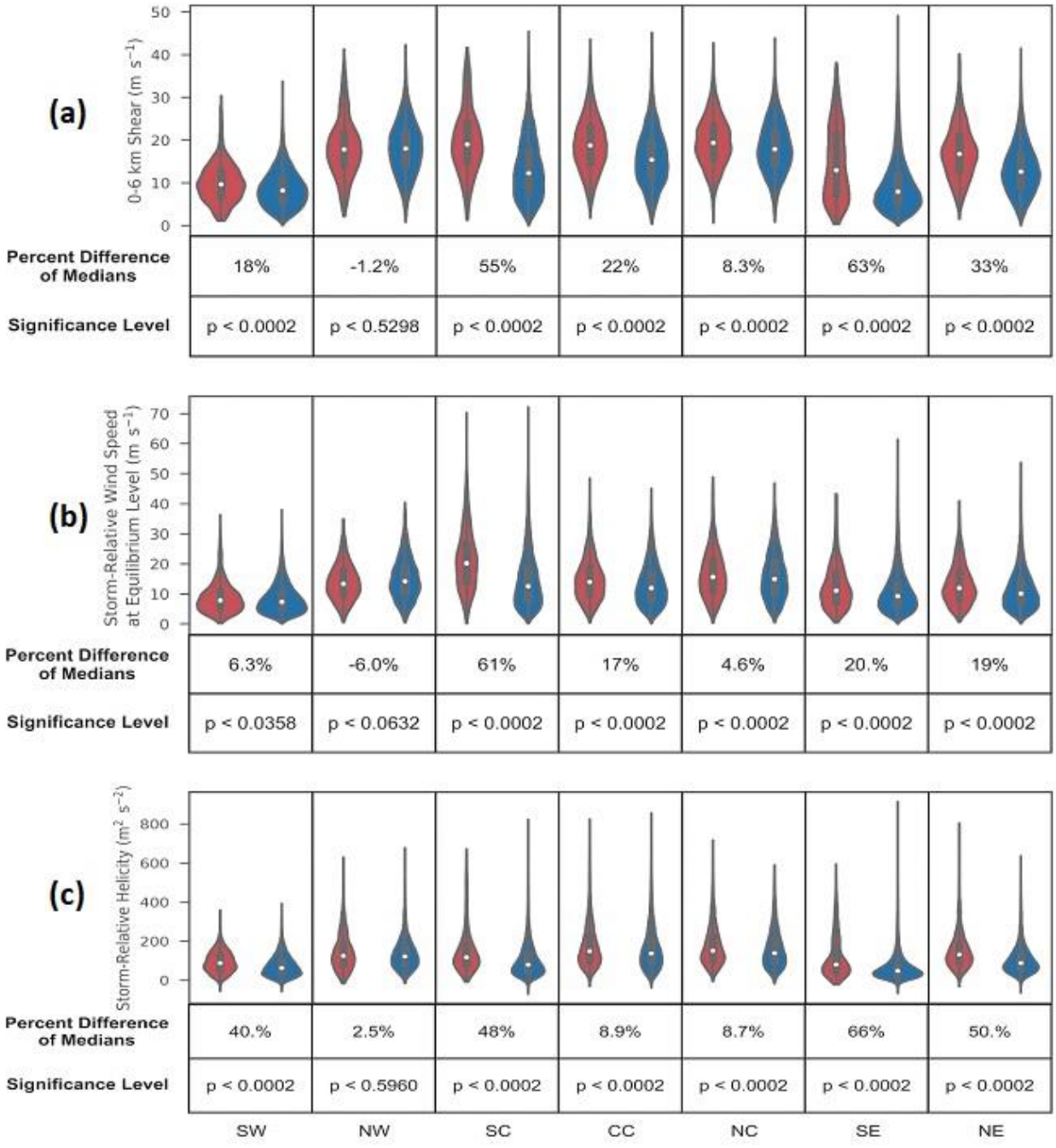

Figure 5. Violin plots of the dynamic variables: (a) 0-6 km shear, (b) storm-relative wind speed at the equilibrium level, and (c) storm-relative helicity for each region. Red (blue) violins correspond to the +CG- (–CG-) dominated cells. See text and caption for Figure 3 for more explanation of the figure.

Figure 5(c) shows the distribution of SRH in environments containing +CG-dominated and –CG-dominated cells in every region. The differences in medians between +CG-dominated and –CG-dominated cells were significant at the 99.98% level in all regions except in the NW region, where the difference was not statistically significant. The southern regions and the NE had the largest percent differences in medians favoring +CG dominated cells. The median value of SRH was greater in +CG-dominated cells than in –CG-dominated cells in every region. As for 0-6 km shear, the percent difference in each southern region was considerably larger than the percent difference in the adjoining region north of it. Furthermore, the largest percent differences were in the easternmost regions, the largest being in the SE, and the second-largest being in the NE. Again, the fact that the difference was not statistically significant in the NW and that the percent difference was relatively small in the CC and NC regions suggests that this parameter is not the only one affecting the dominant polarity of frequent CG flashes (and therefore, affecting the polarity of the charge structure).

5.4. Other Environmental Parameters

In addition to the 10 parameters presented in the above sections, we analyzed equivalent potential temperature θ_e, the equilibrium level (EL), LFC to EL NCAPE, LFC to -20°C NCAPE, 0°C to -20°C CAPE and NCAPE, and 0-3 km shear. NCAPE is CAPE divided by the depth over which it is calculated and gives the average change in CAPE with per meter of ascent of an air parcel. Larger values of CAPE, NCAPE, and 0-3 km shear all might increase SLWC by increasing updraft speed within some layer and might thereby reduce residence time below the middle of the mixed phase region, as discussed previously for other related parameters. θ_e was analyzed because Smith et al. (2000) found that θ_e was smaller in the environments of +CG-dominated storms than in the environments of –CG-dominated storms on analyzed days. EL was chosen because Carey and Buffalo (2007) had found that somewhat lower EL heights were associated with storms in which +CGs constituted relatively high fractions of CG activity (>25% of CGs). The percent difference in medians between +CG dominated cells and –CG-dominated cells is shown for all parameters and regions in Table 2.

The magnitudes of the percent differences in median values of θ_e for +CG-dominated and –CG-dominated cells were extremely small at best, so this parameter will not be discussed further. The relationship with EL was mixed: +CG-dominated cells had a modestly smaller median value of EL than –CG-dominated cells had in the CC region, consistent with the findings of Carey and Buffalo (2007), but had modestly larger median values in the SW and NC. Percent differences in the median values of EL for +CG-dominated and –CG-dominated cells were much smaller (magnitudes <3%) in the SC and SE regions and median ELs were not significantly different in the NW and NE regions. The relationships with the other CAPE parameters were also mixed, but 0°C to -20°C CAPE and NCAPE displayed statistically significant differences between the two types of cells for all regions and favored greater SLWC in the +CG-dominated cells in all regions except the CC region. The relationship with 0-3 km shear was similar to that of SRH and 0-6 km shear in that median values were higher for the +CG-dominated cells in all regions, with the southern regions having higher percent differences. Also as in the case of SRH and 0-6 km shear, the difference in median 0-3 km shear was not significant in the NW region. More details concerning these parameters are available in Eddy (2018).

Table 2. *The percent difference in the median values of each environmental parameter (median for +CG-dominated cells minus the median for –CG dominated cells) in each region, for all seventeen parameters analyzed in this study.*

	SW	NW	SC	CC	NC	SE	NE
WCD	34	30.	-17	-28	19	3.3	-3.4
CBH	-26	-21	16	23	-18	-25	-2.9
DPD	-21	-8.2	10.	35	-19	-24	4.0
PWAT	3.4	-0.54*	-16	-22	6.6	-7.3	-5.6
θ_e	0.73	0.17*	-1.0	-1.1	1.0	-0.65	0.26
LFC to EL CAPE	88	15	28	-8.0	77	1.8*	37
LFC to EL NCAPE	57	8.9*	35	3.4	55	5.7	40.
LFC to -20°C CAPE	60.	18	19	-17	64	-0.54*	28
LFC to -20°C NCAPE	44	8.9*	31	-0.52*	45	2.7*	29
0°C to -20°C CAPE	49	18	35	-4.0	59	5.2	40.
0°C to -20°C NCAPE	48	15	36	-2.9	57	5.9	40.
|CIN|	-1.5*	-24	68	44	-11	31	32
EL	14	2.0*	-2.4	-6.9	9.1	-2.8	0.11*
0-3 km shear	24	1.6*	30.	11	5.9	42	30.
0-6 km shear	18	-1.2*	55	22	8.3	63	33
Storm-relative wind speed at EL	6.3	-6.0	61	17	4.6	20.	19
SRH	40.	2.5*	48	8.9	8.7	66	50.

Note. Cell colors indicate the group to which they belong: green, for moisture parameters; orange, for thermodynamic parameters; and blue, for dynamic parameters. Percent differences that were not significant at ≥ the 90% level are marked with superscript asterisks. Darkness of color indicates three ranges of the magnitude of the percent difference in the median values of environmental parameters hypothesized to favor +CG-dominated cells over –CG-dominated cells through their expected effect on SLWC, from darkest to palest shading: ≥35%, ≥4% & <35%, and <4% or not significantly different or favoring –CG-dominated cells. EL has darker shading for both signs of difference because either could be interpreted as favoring +CG-dominated cells.

6. Discussion and Conclusions

Our goal for this study was to determine which environmental parameters are conducive to storms having anomalous vertical charge distributions across all of CONUS, apart from the regional trends that affect all storms in a given region. The most direct approach, used by Fuchs et al. (2015) would be to use three-dimensional lightning mapping observations which indicate the charge regions involved in lightning flashes. However, such observations are available in only a few locations, so an alternative approach was needed. Our indirect approach, similar to the approaches used on a regional scale by Carey and Buffalo (2007) and by Lang and Rutledge

(2011), was to analyze 11 years of cloud-to-ground (CG) data over CONUS from Vaisala's National Lightning Detection Network (NLDN) under the assumption that storms whose CG activity was strongly dominated by +CG flashes have inverted-polarity charge distributions, as has been observed for many storms in the CC region.

At a minimum, this is the first study to estimate the distribution of warm-season deep-convective storms identified by the NLDN as having moderate to large CG flash rates of either dominant polarity for all of CONUS. Although the threshold for +CG peak currents is what has been recommended by studies that have had verification of +CG identification (e.g., Biagi et al., 2007; Cummins and Murphy, 2009; Calhoun et al., 2013), these studies also found some contamination by intracloud flashes for NDLN-detected +CGs with peak currents between 15 kA and 20 kA (roughly 50% of detected +CGs at 15 kA decreasing to nearly 0% at 20 kA). Actually, these two studies found that NLDN-detected –CG flashes in inverted-polarity storms in the CC region have similar contamination by intracloud flashes over a similar range of peak currents. Another possibility of contamination of +CG-detected NDLN data has been raised by a recent study which found that the NLDN misclassified some compact intracloud discharges (CIDs) as large peak current +CGs (Leal et al., 2019). However, the reverse relationship, the fraction of NLDN-detected +CGs that are really CIDs, may be small, and previous studies (MacGorman and Taylor, 1989; Biagi et al., 2007; Fleenor et al., 2009) provide evidence that this is the case, as discussed in Section 3.

As a study of inverted-polarity storms, our conclusions have some caveats:

(1) As described in Section 3, we attempted to reduce double counting of cells by eliminating duplicates that overlapped in time or space. If two cells partially overlapped in space and occurred within 30 minutes of each other, only the cell with the greatest number of CG flashes was kept for analysis. Even so, some pairs of storm cells in the dataset likely were not statistically independent, which would artificially inflate significance levels. However, because most of the significance levels for median differences in environmental parameters for +CG-dominated cells and –CG-dominated cells were very high, it is likely that many of the relationships found in this study would still exhibit a high degree of significance even if any remaining dependence between cells were completely removed.

(2) Our intent in using a much higher and a much lower threshold for the fraction of CGs composed of +CGs than has been used in studies previously was to make it much more likely that the storm cells included in our study had inverted- or normal-polarity vertical charge distributions. We also limited the time of year and time of day to minimize the contamination by winter storms and by the stratiform region of MCSs, in which CG activity can be dominated by +CG flashes for much different reasons. Previous studies (e.g., Calhoun et al., 2013; DiGangi et al., 2016; Lang et al., 2011; Rust et al., 2005) have provided a substantial data base of +CG-dominated storms in the CC region that had inverted-polarity vertical charge distributions, but the relationship between +CG domination and vertical charge structure is only hypothesized elsewhere. Verifying the relationship elsewhere will require in-storm soundings of electric fields or three-dimensional lightning mapping observations in conjunction with systems that continuously map ground strikes. Because the NC region has a large number of suitable storms (Table 1), a field program there would likely succeed. It will be much more difficult in the southern regions, where suitable storms constitute a small percentage of storms, and would be most difficult in the

NW where they are rarest. Although our conclusions regarding anomalous charge distributions outside the CC region are based on a hypothesized relationship with +CG domination and so are subject to verification, results concerning the environments of +CG-dominated storms themselves are still valid. This is the first CONUS-wide analysis of environmental conditions under which +CG flashes constitute a supermajority of CGs in storm cells having moderate to large CG flash rates.

The geographic distribution of cells satisfying our criteria is shown in Figure 2. To analyze what geographic patterns in the environmental conditions favoring +CG-dominated cells over –CG-dominated cells, we divided CONUS into seven regions (Fig. 1). The result by region, shown in Table 1, is that the CC and NC regions each had more than twice as many +CG dominated cells as any other region. Overall, the total number of cells analyzed in each region increased in regions going from north to south and from west to east, while the fraction of analyzed cells satisfying the criteria for +CG-dominated cells increased from south to north and was largest by far in the north-central region (59%) and the central-central region (25%). These geographic trends roughly parallel what has been published in climatologies of the distribution of +CG flashes and –CG flashes in the CONUS (e.g., Boccippio et al. 2001; Orville et al., 1987, 2001), but here the distributions are for cells, not individual flashes, with each analyzed cell having moderate to large CG flash rates dominated by a large fraction of either +CG or –CG flashes. Note that the north-central region was the only region in which cells satisfying our criteria for +CG-dominated cells outnumbered cells satisfying our criteria for –CG-dominated cells. Cells in which +CGs dominated CG activity constituted <4% of analyzed cells in all three southern regions and <1% in the SE.

We analyzed the distribution of seventeen environmental parameters in each region to determine the median value of each parameter for +CG-dominated cells and for –CG-dominated cells. As described in Section 5, these parameters were selected because one or more previous studies had hypothesized that they could influence the supercooled liquid water content (SLWC, supercooled droplets) in the mixed-phase region of updrafts. Laboratory studies have shown that rebounding collisions between graupel and small ice particles in the presence of large SLWC causes the graupel to gain positive charge when exchanging charge with cloud ice, rather than gaining the usual negative charge, and would cause the polarity of the storm's vertical charge distribution to be inverted from the usual polarity (with the resulting CG flashes being dominated by +CG flashes). Table 2 shows the percent difference in median values for each parameter in each region between storms dominated by +CG flashes and those dominated by –CG flashes. Differences hypothesized to favor +CG-dominated cells are highlighted by fuller color.

To highlight the variations from region to region, Table 3 shows the environmental parameters that are consistent with the hypothesized effect on supercooled liquid water content in each region, ordered from the largest to smallest percent difference in median values. The wide variety across various regions suggests that anomalous charge distributions can be produced by a variety of combinations of environmental factors, the lack of one or more factors conducive to anomalous distributions in a region being offset by other factors.

Table 3. *Environmental parameters favoring +CG-dominated cells in each of seven regions spanning CONUS, in descending order of the magnitude of the percent difference in median values between +CG- and -CG-dominated cells*

SW	NW	SC	CC	NC	SE	NE
LFC to EL CAPE	LFC to −20°C CAPE	|CIN|	|CIN|	LFC to EL CAPE	SRH	SRH
LFC to −20°C CAPE	0°C to −20°C CAPE	storm-relative wind at EL	DPD	LFC to −20°C CAPE	0–6 km shear	0°C to −20°C CAPE
LFC to EL NCAPE	LFC to EL CAPE	0–6 km shear	WCD	0°C to −20°C CAPE	0–3 km shear	0°C to −20°C NCAPE
0°C to −20°C CAPE	0°C to −20°C NCAPE	SRH	CBH	0°C to −20°C NCAPE	|CIN|	LFC to EL NCAPE
0°C to −20°C NCAPE		0°C to −20°C NCAPE	PWAT	LFC to EL NCAPE	Storm-relative wind at EL	LFC to EL CAPE
LFC to −20°C NCAPE		0°C to −20°C CAPE	0–6 km shear	LFC to −20°C NCAPE	PWAT	0–6 km shear
SRH		LFC to EL NCAPE	Storm-relative wind at EL	EL height	0°C to −20°C NCAPE	|CIN|
0–3 km shear		LFC to −20°C NCAPE	0–3 km shear	SRH	LFC to EL NCAPE	0–3 km shear
0–6 km shear		0–3 km shear	SRH	0–6 km shear	0°C to −20°C CAPE	LFC to −20°C NCAPE
EL height		LFC to EL CAPE	EL height	0–3 km shear		LFC to −20°C CAPE
Storm-relative wind at EL		LFC to −20°C CAPE		Storm-relative wind at EL		Storm-relative wind at EL
		WCD				PWAT
		CBH				DPD
		PWAT				
		DPD				

Note: Color shading indicates ranges of the magnitude of the percent difference in medians for parameters with significance levels ≥90%, in descending order from gold, to red, to turquoise, to violet, respectively: ≥50%, <50% & ≥35%, <35% & ≥15%,<15% & ≥4%. See Table 2 for the percent difference values.

The CC region had the largest sample of +CG-dominated cells that made it through the filtering process and is the most-studied region for environmental effects on dominant CG polarity and/or a storm's vertical charge structure (e.g., Carey & Buffalo, 2007; Lang & Rutledge, 2011; Lang et al., 2004; MacGorman et al., 2005; Rust & MacGorman, 2002; Rust et al., 2005; Tessendorf et al., 2007a, 2007b; Weiss et al., 2008; Wiens et al., 2005). While all of the moisture parameters in the CC region had moderate to large percent differences in median values favoring enhanced SLWC in the +CG-dominated storms, the largest percent difference was for |CIN|, a thermodynamic parameter. The only other thermodynamic parameter favoring +CG-dominated cells was LFC to EL NCAPE, although not by much (3.4%). All of the dynamic parameters favored +CG-dominated cells, although most of their magnitudes of percent difference were smaller than for the moisture parameters.

The NC region had the second-largest number of +CG-dominated cells and was the only region to have more +CG-dominated cells than –CG-dominated cells satisfying flash rate and percentage thresholds. Yet, unlike the CC region, all of the moisture parameters favored greater

SLWC in –CG-dominated cells rather than in +CG-dominated cells. However, all of the CAPE and NCAPE parameters had large percent differences in median parameter values favoring greater SLWC in the +CG-dominated cells, and all of the dynamic parameters favored it as well, although with percent differences that were <10%.

The SC region was unique in that all the analyzed environmental parameters had percent differences in medians definitively favoring greater SLWC in +CG dominated cells except the height of the EL. As in the CC region, the largest percent difference was for |CIN|, and it was the only other region in which all of the moisture parameters favored greater SLWC in the +CG-dominated cells, although with smaller percent differences than most dynamic and thermodynamic parameters had there. Storm-relative wind speed at the EL was second only to |CIN|, followed closely by two other dynamic parameters; the percent differences for the dynamic parameters in the SC were greater than in most regions.

In the SE region, only PWAT of the moisture parameters and only three of the six parameters related to CAPE favored +CG-dominated cells, but all of them had relatively small percent differences. |CIN| was the only thermodynamic parameter with a moderately large percent difference favoring +CG-dominated cells. The largest favorable percent differences were for three of the dynamic parameters, which also had larger percent differences in the SE than in all other regions.

In the NE region, as in the SE region, SRH was the environmental parameter having the largest percent difference favoring greater SLWC in +CG dominated storms, but unlike the SE region, four of the CAPE-related parameters also had large percent differences. A mixture of dynamic parameters and thermodynamic parameters had moderate percent differences favoring +CG-dominated storms, while only two moisture parameters had favorable percent differences with magnitude greater than 4%.

The environmental parameters favoring +CG-dominated cells in the SW region were the same as those in the NC region, with all CAPE related parameters having a larger percent difference than all the dynamic parameters. Percent differences in the SW were larger than in the NC for all the dynamic parameters (particularly for SRH) and were slightly smaller than in the NC for most thermodynamic parameters. However, the largest percent difference favoring greater SLWC in any region and for any parameter was the 88% for LFC to EL CAPE in the SW.

Compared to all other regions, the NW region had the smallest number of cells for both dominant polarities of CGs (Table 1), consistent with its having the smallest median values of LFC to EL CAPE and of LFC to −20°C CAPE. It also had the fewest environmental parameters favoring +CG-dominated cells. The difference in medians for the moisture and dynamic parameters all either favored greater SLWC in the –CG-dominated cells or were not significantly different. The only parameters with statistically significant differences favoring +CG-dominated cells were four of the six CAPE-related parameters, and those percent differences were all <20%. Thus, while there were thermodynamic factors favoring greater SLWC for +CG-dominated cells to compensate for the lack of favorable moisture and dynamic parameter values, the compensating factors were fewer and weaker than in any of the other regions.

Previous studies of environmental parameters associated with storms having unusually large +CG fractions of CG flash activity have all involved parts of the CC region. In Kansas, Oklahoma, and the Texas panhandle, for example, Carey and Buffalo (2007) found that storms in which +CGs composed >25% of CGs were associated with: shallower WCD, higher CBH, lower PWAT, greater DPD, greater 0-3 km shear, greater 0-3 km SRH, a lower EL, and greater LFC to EL NCAPE than storms in which +CGs composed <25%. However, unlike this study, they found that such storms were associated with less |CIN|, and they did not find statistically significant differences for LFC to EL CAPE, storm-relative wind speed at the EL, or 0-6 km shear. Similarly, Lang and Rutledge (2011) found that storms having ≥50% +CGs in the STEPS region occurred in environments with greater 0-3 km shear, greater 0-6 km wind shear, and greater SRH than storms having <50% +CGs, much as we observed. However, unlike our results in the CC region, which includes the STEPS region, they found that storms satisfying their criteria for +CGs were associated with environments having much greater LFC to EL CAPE, slightly lower CBHs, slightly deeper WCDs, and higher storm tops (inferred here as also meaning a higher EL).

Rather than analyzing CG data, Fuchs et al. (2015) studied LMA data to infer anomalous and normal storm charge distributions based on the height of positive charge inferred from mapped lightning flashes. They compared the environments of anomalous and normal polarity storms in Oklahoma and in northeastern Colorado, as well as in two other locations in which they found no storms with anomalous charge distribution. In Oklahoma, the environments of anomalously polarized storms had larger LFC to EL NCAPE than in Colorado, where they had smaller values of NCAPE, but had higher CBHs and larger N40 aerosol concentrations. We did not study aerosols, but their observation of higher CBHs and smaller NCAPE in Colorado agrees with our results for the CC region. Although both of the regions for which they analyzed anomalous charge distributions are within our CC region, the fraction of storms with anomalous vertical polarity tends to be larger in Colorado than in Oklahoma. Note that Lang and Rutledge (2011) analyzed essentially the same region as for the Colorado storms in Fuchs et al. (2015). Although they selected storms on the basis of CG data, they also analyzed LMA data and inferred that storms satisfying their +CG criteria tended to be anomalously polarized. At least some of the difference in results from Fuchs et al. and Lang et al. may be from their different approaches. Lang et al. examined the differences between their two categories of storms in the same region, while Fuchs et al. concentrated on the differences in environments favoring +CG-dominated storms in Colorado compared with other regions. When Fuchs et al. considered storms solely in Colorado, the only differences between the two categories they found were that storms with anomalous charge distributions had larger N40 aerosol concentrations and storms with normal charge distributions had greater NCAPE.

Note that the differences in methodology, regions, and periods analyzed among these studies and between these studies and our study could all affect the differences in the environmental properties they identified as distinguishing between storms with anomalous charge distributions or larger +CG fractions and storms with normal charge distributions or smaller +CG fraction. Furthermore, one should be somewhat cautious when interpreting our results in Table 3 as being a list of the necessary ingredients in each region. It is possible, for example, that the influence of moisture parameters in the CC region may have been due in part to the geographic distributions of the two categories of storm cells: Figure 1 shows that the northern part of the CC region had much larger numbers of +CG-dominated cells than the southern portion, while the southern

portion had much larger numbers of –CG-dominated cells. The northern portion tends to have higher cloud base heights and shallower warm cloud depths than the southern region, according to Fuchs et al. (2015). Thus, as suggested by the findings of Lang and Rutledge (2011) and Fuchs et al. (2015), the importance given to moisture parameters in the CC region in our study may have been due more to the climatological difference in the moisture parameters between the northern and southern parts of the region rather than due to differences that would be valid across the northern part of the CC region alone.

Similarly, the lack of a strong impact by a particular parameter does not necessarily mean that the parameter is always unimportant. It is possible that climatological differences in that parameter for all storms in a region may interact with other environmental parameters to allow differences in the other parameters to contribute to producing +CG-dominated storms, even if variations in the parameter itself provide little or no discrimination between +CG-dominated and –CG-dominated storms within the region. The NW region, for example, had median values of CBH and WCD that were even higher and lower, respectively, than in the CC region, although the medians of these parameters in the NW appeared even more conducive to greater SLWC for –CG-dominated storms. It is possible that most storms in the NW region have high enough cloud base heights and small enough warm-cloud depths to aid the relatively small differences in CAPE-related parameters that favor +CG-dominated cells, even though our hypotheses regarding the impact of CBH and WCD alone does not favor such storms when restricted to that region. What our results do suggest, however, is that particular CBH and WCD values are insufficient in themselves to contribute to +CG-dominated cells without the interaction of other parameters.

Additionally, other parameters not explored in this study likely influence the dominant polarity of a storm cell. For example, Fuchs et al. (2015) found that that anomalously charged thunderstorms in Colorado had greater aerosol concentrations and hypothesized that the higher concentrations of cloud condensation nuclei led to smaller drop sizes, which reduced collision-coalescence processes. The link between inverted-polarity storms and greater aerosol concentrations has been inferred outside of the United States as well. Pawar and Kamra (2009) found that storms with inverted-polarity charge structure in India during the drier pre-monsoon season likely had greater aerosol concentrations, in addition to higher CBHs and greater DPDs. All of the inverted-polarity thunderstorms analyzed in Pawar et al. (2017) occurred on days with greater aerosol optical depth than those days with normal-polarity storms. Ammonia concentration may be another factor. Marchand et al. (2019) found that regions of the CONUS with greater ammonia emissions coincided with local maxima in inverted-polarity IC flashes.

In summary, this was the first CONUS-wide analysis of storms cells producing moderate to large CG flash rates dominated by large percentages (≥80%) of +CG flashes, which we inferred to have anomalous charge distributions whose vertical polarity was inverted from the usual polarity. Such storm cells were identified in all regions we analyzed, although most were in the central and north-central United States. In the ensemble of storms including these +CG-dominated cells and cells having large CG flash rates dominated by –CG flashes, +CG-dominated cells constituted 25% of the storm cells in the central region and 59% in the north central region, but less than 4% in most other regions.

We analyzed 17 parameters in the near-storm environment of these storms in seven regions spanning CONUS, seeking to identify environmental characteristics conducive to +CG-dominated storm cells and, by inference, to inverted-polarity storms. These parameters were divided among moisture, thermodynamic, and dynamic parameters, all of which were hypothesized to be capable of contributing to anomalous charge distributions by increasing the SLWC in storm updrafts. We found, in agreement with previous studies of limited regions, that no single environmental parameter or consistent set of environmental parameters characterizes the near-storm environments of +CG-dominated storms across all regions. Parameters that appeared to be strongly associated with +CG-dominated storms in some regions were not associated with +CG-dominated storms at all in other regions. It appears that a parameter that is favorable in one region can compensate for other parameters that are unfavorable in allowing the development and maintenance of inverted-polarity storms.

Nevertheless, if one considers the environmental parameters in Tables 2 and 3 in similar groups in various regions, rather than considering the specific parameters within the groups, either a thermodynamic parameter or a dynamic parameter provided the largest percent difference favoring +CG-dominated cells for every region. There were also some broader regional trends: In the western and northern regions, one of the forms of CAPE provided among the largest percent differences. In the southeast and northeast regions, at least one of the dynamic parameters had among the largest percent differences, and storm-relative helicity best distinguished between +CG-dominated cells and –CG-dominated cells. In the SC region all of the moisture and dynamic parameters and all of the thermodynamic parameters except for EL height had moderate to large magnitudes of percent difference. In the CC region, the moisture parameters on average had the largest magnitudes of percent difference, but this region and the SC region were the only regions in which all of the moisture parameters favored +CG-dominated cells. Overall, it appears that parameters favoring stronger storm updrafts in some way are important in producing +CG-dominated storms and, by inference, inverted polarity storms, as was suggested by Williams et al. (2005).

Acknowledgements

The National Lightning Detection Network data used in this study were from Vaisala and are available from that company. North America Regional Reanalysis data are available from NOAA/ESRL at https://www.esrl.noaa.gov/psd/data/gridded/data.narr.html. The authors thank Kristin Calhoun for providing the scripts that we modified to create the violin plots, Jason Furtado and Michael Richman for helping with the statistical analysis, and Conrad Ziegler for providing the script to perform the Lambert Conformal projection. Funding for this study was provided by NSF grants AGS-1063945 and AGS-1523331. Funding was also provided by NOAA/Office of Oceanic and Atmospheric Research under NOAA-University of Oklahoma Cooperative Agreement #NA11OAR4320072, U.S. Department of Commerce.

References

Alpha, T. R., & Snyder, J. P. (1982). *The properties and uses of selected map projections*. United States Geological Survey. Retrieved from https://pubs.usgs.gov/pp/1395/plate-1.pdf

Baker, B., Baker, M. B., Jayaratne, E. R., Latham, J., & Saunders, C. P. (1987). The influence of diffusional growth rates on the charge transfer accompanying rebounding collisions between ice crystals and soft hailstones. *Quarterly Journal of the Royal Meteorological Society*, *113*, 1193-1215. doi:10.1002/qj.49711347807

Biagi, C. J., Cummins, K. L., Kehoe, K. E., Krider, E. P. (2007). National Lightning Detection (NLDN) performance in southern Arizona, Texas, and Oklahoma in 2003–2004. *Journal of Geophysical Res*earch, *112*, D05208. doi:10.1029/2006JD007341.

Boccippio, D. J., Cummins, K. L., Christian, H. J., & Goodman, S. J. (2001). Combined satellite- and surface-based estimation of the intracloud–cloud-to-ground lightning ratio over the continental United States. *Monthly Weather Review*, *129*, 108–122. https://doi.org/10.1175/1520-0493(2001)129<0108:CSASBE>2.0.CO;2

Branick, M. L., & Doswell, C. A., III (1992). An observation of the relationship between supercell structure and lightning ground strike polarity. *Weather and Forecasting, 7*, 143–149.

Brook, M., Nakano, M., Krehbiel, P., & Takeuti, T. (1982). The electrical structure of the Hokuriku winter thunderstorms. *Journal of Geophysical Research*, *87*(C2), 1207–1215. https://doi.org/10.1029/JC087iC02p01207

Bruning, E. C., Weiss, S. A., & Calhoun, K. M. (2014). Continuous variability in thunderstorm primary electrification and an evaluation of inverted-polarity terminology. *Atmospheric Research*, *135–136*(2014), 274–284. https://doi.org/10.1016/j.atmosres.2012.10.009

Calhoun, K. M., Macgorman, D. R., Ziegler, C. L., & Biggerstaff, M. I. (2013). Evolution of lightning activity and storm charge relative to dual-Doppler analysis of a high-precipitation supercell storm. *Monthly Weather Review*, *141*(7), 2199–2223. https://doi.org/10.1175/MWR-D-12-00258.1

Carey, L. D., & Buffalo, K. M. (2007). Environmental control of cloud-to-ground lightning polarity in severe storms. *Monthly Weather Review*, *135*(4), 1327–1353. https://doi.org/10.1175/MWR3361.1

Clarence, N. D., & Malan, D. J. (1957). Preliminary discharge processes in lightning flashes to ground. *Quarterly Journal of the Royal Meteorological Society*, *83*(356), 161–172. https://doi.org/10.1002/qj.49708335603

Cooray, V. (2015). An Introduction to Lightning. Springer. https://doi.org/10.1007/978-94-017-8938-7

Cummins, K. L., & Murphy, M. J. (2009). An overview of lightning locating systems: History,

techniques, and data uses, with an in-depth look at the U.S. NLDN. *IEEE Transactions on Electromagnetic Compatibility*, *51*(3), 499–518. https://doi.org/10.1109/TEMC.2009.2023450

Curran, E. B., & Rust, W. D. (1992). Positive ground flashes produced by low-precipitation thunderstorms in Oklahoma on 26 April 1984. *Monthly Weather Review, 120,* 544-553.

DiGangi, E. A., MacGorman, D. R., Ziegler, C. L., Betten, D., Biggerstaff, M., Bowlan, M., & Potvin, C. (2016). An overview of the 29 May 2012 Kingfisher supercell during DC3. *Journal Geophysical Research: Atmospheres,* 121, 14316–14343. doi:10.1002/2016JD025690

Eddy, A. J., (2018). *Environmental conditions producing thunderstorms with anomalous vertical polarity of charge structure* (Master's Thesis). Retrieved from SHAREOK. (https://hdl.handle.net/11244/299935). Norman, OK: The University of Oklahoma.

Emersic, C., & Saunders, C. P. R. (2010). Further laboratory investigations into the Relative Diffusional Growth Rate theory of thunderstorm electrification. *Atmospheric Research, 98,* 327–340. doi:10.1016/j.atmosres.2010.07.011

Fleenor, S. A., Biagi, C. J., Cummins, K. L., Krider, E. P., & Shao, X. M. (2009). Characteristics of cloud-to-ground lightning in warm-season thunderstorms in the Central Great Plains. *Atmospheric Research, 91*(2009), 333–352. https://doi.org/10.1016/j.atmosres.2008.08.011

Fuchs, B. R., Rutledge, S. A., Bruning, E. C., Pierce, J. R., Kodros, J. K., Lang, T. J., et al. (2015). Environmental controls on storm intensity and charge structure in multiple regions of the continental United States. *Journal of Geophysical Research: Atmospheres*, *120*(13), 6575–6596. https://doi.org/10.1002/2015JD023271

Fuchs, B. R., Rutledge, S. A., Dolan, B., Carey, L. D., & Schultz, C. (2018). Microphysical and kinematic processes associated with anomalous charge structures in isolated convection. *Journal of Geophysical Research: Atmospheres, 123,* 6505–6528. https://doi.org/10.1029/2017JD027540

Gilmore, M. S., & Wicker, L. J. (2002). Influences of the local environment on supercell cloud-to-ground lightning, radar characteristics, and severe weather on 2 June 1995*. *Monthly Weather Review*, *130*(10), 2349–2372. https://doi.org/10.1175/1520-0493(2002)130<2349:IOTLEO>2.0.CO;2

Helsdon, J. H., Jr., Wojcik, W. A. & Farley R. D. (2001). An examination of thunderstorm-charging mechanisms using a two-dimnsional storm electrification model. *Journal of Geophysical Research, 106,* 1165–1192.

Jacobson, E. A., & Krider, E. P. (1976). Electrostatic field changes produced by Florida lightning. *Journal of the Atmospheric Sciences, 33,* 103–117, https://doi.org/10.1175/1520-0469(1976)033<0103:EFCPBF>2.0.CO;2

Jayaratne, E. R., & Saunders, C. P. R. (1984). The “rain gush”, lightning, and the lower positive charge center in thunderstorms. *Journal of Geophysical Research: Atmospheres*, *89*(D7), 11816–

11818. https://doi.org/10.1029/JD089iD07p11816

Jayaratne, E. R., Saunders, C. P. R., & Hallett, J. (1983). Laboratory studies of the charging of soft-hail during ice crystal interactions. *Quarterly Journal of the Royal Meteorological Society*, *109*(461), 609–630. https://doi.org/10.1002/qj.49710946111

Knapp, D. I. (1994). *Using cloud-to-ground lightning data to identify tornadic thunderstorm signatures and nowcast severe weather*. White Sands Missile Range, NM: US Army Research Laboratory.

Krider, E. P., Noggle, R. C., Pifer, A. E., & Vance, D. L. (1980). Lightning direction-finding systems for forest fire detection. *Bulletin of the American Meteorological Society*, *61*, 980–986.

Lang, T. J., Miller, L. J., Weisman, M., Rutledge, S. A., Barker, L. J., Bringi, V. N., et al. (2004). The severe thunderstorm electrification and precipitation study. *Bulletin of the American Meteorological Society*, *85*(8), 1107–1125. https://doi.org/10.1175/BAMS-85-8-1107

Lang, T. J., & Rutledge, S. A. (2011). A framework for the statistical analysis of large radar and lightning datasets: Results from STEPS 2000. *Monthly Weather Review*, *139*(8), 2536–2551. https://doi.org/10.1175/MWR-D-10-05000.1

Leal, A. F. R., Rakov, V. A., Rocha, B. R. P. (2019). Compact intracloud discharges: New classification of field waveforms and identification by lightning locating systems. *Electric Power Systems Research*, *173*(2019), 251–262. https://doi.org/10.1016/j.epsr.2019.04.016

MacGorman, D. R., Apostolakopoulos, I. R., Lund, N. R., Demetriades, N. W. S., Murphy, M. J., & Krehbiel, P. R. (2011). The timing of cloud-to-ground lightning relative to total lightning activity. *Monthly Weather Review*, *139*(12), 3871–3886. https://doi.org/10.1175/MWR-D-11-00047.1

MacGorman, D. R., & Burgess, D. W. (1994). Positive cloud-to-ground lightning in tornadic storms and hailstorms. *Monthly Weather Review*, *122*(8), 1671–1697. https://doi.org/10.1175/1520-0493(1994)122<1671:PCTGLI>2.0.CO;2

MacGorman, D. R., Elliott, M. S., & DiGangi, E. (2017). Electrical discharges in the overshooting tops of thunderstorms. *Journal of Geophysical Research: Atmospheres*, *122*(5), 2929–2957. https://doi.org/10.1002/2016JD025933

MacGorman, D. R., & Morgenstern, C. D. (1998). Some characteristics of cloud-to-ground lightning in mesoscale convective systems. *Journal of Geophysical Research*, 103, 14011–14023.

MacGorman, D. R., & Rust, W. D. (1998). *The Electrical Nature of Storms*, New York, NY: Oxford University Press.

MacGorman, D. R., Rust, W. D., Krehbiel, P., Rison, W., Bruning, E., & Wiens, K. (2005). The

electrical structure of two supercell storms during STEPS. *Monthly Weather Review*, *133*(9), 2583–2607. https://doi.org/10.1175/MWR2994.1

MacGorman, D. R., Rust, W. D., Schuur, T. J., Biggerstaff, M. I., Straka, J. M., Ziegler, Z. L., et al. (2008). TELEX The thunderstorm electrification and lightning experiment. *Bulletin of the American Meteorological Society*, *89*, 997-1014. https://doi.org/10.1175/2007BAMS2352.1

MacGorman, D. R., & Taylor, W. L. (1989). Positive cloud-to-ground lightning detection by an LLP direction-finder network. *Journal of Geophysical Research*, *94*, 13313–13318.

Maddox, R. A., Howard, K. W., Bartels, D. L., & Rodgers, D. M. (1986). Mesoscale convective complexes in the middle latitudes. In P. S. Ray (Ed.), *Mesoscale Meteorology and Forecasting, American Meteorological Society* (pp 390-413). Boston, MA. https://doi.org/10.1007/978-1-935704-20-1_17

Makowski, J. A., MacGorman, D. R., Biggerstaff, M. I., & Beasley, W. H. (2013). Total lightning characteristics relative to radar and satellite observations of Oklahoma mesoscale convective systems. *Monthly Weather Review*, *141*(5), 1593–1611. https://doi.org/10.1175/MWR-D-11-00268.1

Mansell, E. R., MacGorman, D. R., Ziegler, C. L., & Straka, J. M. (2002). Simulated three-dimensional branched lightning in a numerical thunderstorm model. *Journal of Geophysical Research: Atmospheres*, *107*(D9). https://doi.org/10.1029/2000JD000244

Mansell, E. R., MacGorman, D. R. Ziegler, C. L. & Straka, J. M. (2005). Charge structure in a simulated multicell thunderstorm. *Journal of Geophysical Research, 110*, D12101. doi:10.1029/2004JD005287

Mansell, E. R., Ziegler, C. L., & Bruning, E. C. (2010). Simulated electrification of a small thunderstorm with two-moment bulk microphysics. *Journal of the Atmospheric Sciences, 67*, 171–194. doi:10.1175/2009JAS2965.1

Marchand, M., Hilburn, K., & Miller, S. D. (2019). Geostationary Lightning Mapper and Earth Networks Lightning Detection over the contiguous United States and dependence on flash characteristics. *Journal of Geophysical Research: Atmospheres*, 124. https://doi.org/10.1029/2019JD031039

Medici, G., Cummins, K. L., Cecil, D. J., Koshak, W. J., & Rudlosky, S. D. (2017). The intracloud lightning fraction in the contiguous United States. *Monthly Weather Review*, *145*(11), 4481–4499. https://doi.org/10.1175/MWR-D-16-0426.1

Mesinger, F., DiMego, G., Kalnay, E., Mitchell, K., Shafran, P. C., Ebisuzaki, W., et al. (2006). North American Regional Reanalysis. *Bulletin of the American Meteorological Society*, *87*(3), 343–360. https://doi.org/10.1175/BAMS-87-3-343

Nag, A., Murphy, M. J., & Cramer, J. A. (2016). *Update to the U.S. National Lightning*

Detection Network. Paper presented at 24th International Lightning Detection Conference (ILDC), San Diego, CA.

NCAR/UCAR. (2019). Research Data Archive: Computational & Information Systems Lab. Retrieved February 3, 2018, from rda.ucar.edu

Orville, R. E. (2008). Development of the National Lightning Detection Network. *Bulletin of the American Meteorolical Society, 89,* 180–190. https:doi.org/10.1175/BAMS-89-2-180

Orville, R. E., & Huffines, G. R. (2001). Cloud-to-ground lightning in the United States: NLDN results in the first decade. 1989–98. *Monthly Weather Review, 129,* 1179–1193.

Orville, R. E., Weisman, R. A., Pyle, R. B., Henderson, R. W., & Orville, R. E., Jr. (1987). Cloud-to-ground lightning flash characteristics from June 1984 through May 1985. *Journal of Geophysical Research, 92,* 5640–5644.

Pawar, S. D., Gopalakrishnan, V., Murugavel, P., Veremey, N. E., & Sinkevich, A. A. (2017). Possible role of aerosols in the charge structure of isolated thunderstorms. *Atmospheric Research, 183,* 331–340. https://doi.org/10.1016/j.atmosres.2016.09.016

Pawar, S. D., & Kamra, A. K. (2009). Maxwell current density characteristics below isolated thunderstorms in tropics. *Journal of Geophysical Research, 114.*

Rasmussen, K., & Houze, R. Jr. (2016). Convective initiation near the Andes in subtropical South America. *Monthly Weather Review*, *144*(6), 2351– 2374.

Rasmussen, E. N., & Straka, J. M. (1998). Variations in supercell morphology. Part I: Observations of the role of upper-level storm-relative flow. *Monthly Weather Review*, *126*, 2406–2421.

Reap, R. M., & MacGorman, D. R., (1989). Cloud-to-ground lightning: Climatological characteristics and relationship to model fields, radar observations, and severe local storms. *Monthly Weather Review*, *117*, 518–535.

Rudlosky, S. D., & Fuelberg, H. E. (2011). Seasonal, regional, and storm-scale variability of cloud-to-ground lightning characteristics in Florida. *Monthly Weather Review*, *139*(6), 1826–1843. https://doi.org/10.1175/2010MWR3585.1

Rust, W. D., & MacGorman, D. R. (2002). Possibly inverted-polarity electrical structures in thunderstorms during STEPS. *Geophysical Research Letters*, *29*(12). https://doi.org/10.1029/2001GL014303

Rust, W. D., MacGorman, D. R., Bruning, E. C., Weiss, S. A., Krehbiel, P. R., Thomas, R. J., et al. (2005). Inverted-polarity electrical structures in thunderstorms in the Severe Thunderstorm Electrification and Precipitation Study (STEPS). *Atmospheric Research*, *76*(2005), 247–271. https://doi.org/10.1016/j.atmosres.2004.11.029

Rutledge, S. A., & MacGorman, D. R. (1988). Cloud-to-ground lightning activity in the 10–11 June 1985 mesoscale convective system observed during the Oklahoma–Kansas PRE-STORM project. *Monthly Weather Review*, *116*(7), 1393–1408. https://doi.org/10.1175/1520-0493(1988)116<1393:CTGLAI>2.0.CO;2

Rutledge, S. A., Williams, E. R., & Petersen, W. A. (1993). Lightning and electrical structure of mesoscale convective systems. *Atmospheric Research*, *29*(1993), 27–53. https://doi.org/10.1016/0169-8095(93)90036-N

Saunders, C. P. R., Keith, W. D., & Mitzeva, R. P. (1991). The effect of liquid water on thunderstorm charging. *Journal of Geophysical Research: Atmospheres*, *96*(D6), 11007–11017.

Saunders, C. P. R., & Peck, S. L. (1998). Laboratory studies of the influence of the rime accretion rate on charge transfer during crystal/graupel collisions. *Journal of Geophysical Research: Atmospheres*, *103*(D12), 13949–13956.

Seimon, A. (1993). Anomalous cloud-to-ground lightning in an F5-tornado-producing supercell thunderstorm on 28 August 1990. *Bulletin of the American Meteorological Society*, *74*, 189–203.

Shao, X. M., Stanley, M., Regan, A., Harlin, J., Pongratz, M., Stock, M. (2006). Total lightning observations with the new and improved Los Alamos Sferic Array (LASA). *Journal of Atmospheric and Oceanic Technology*, *23*, 1273–1288.

Simpson, G., & Robinson, G. D. (1941). The distribution of electricity in thunderclouds, II. In *Proceedings of the Royal Society A: Mathematical, Physical and Engineering Sciences* (Vol. 177, pp. 281–329). The Royal Society. https://doi.org/10.1098/rspa.1941.0013

Smith, S. B., LaDue, J. G., & MacGorman, D. R. (2000). The relationship between cloud-to-ground lightning polarity and surface equivalent potential temperature during three tornadic outbreaks. *Monthly Weather Review*, *128*, 3320–3328. https://doi.org/10.1175/1520-0493(2000)128<3320:TRBCTG>2.0.CO;2

Snyder, J. P. (1987). *Map projections: A working manual*. *U.S. Geological Survey Professional Paper 1395*. Washington: U.S. Government Printing Office. https://doi.org/10.2307/1774978

Stolzenburg, M., Rust, W. D., & Marshall, T. C. (1998). Electrical structure in thunderstorm convective regions: 3. Synthesis. *Journal of Geophysical Research*, *103*(D12), 14097–14108. https://doi.org/10.1029/97JD03545

Takagi, N., Takeuti, T., & Nakai, T. (1986). On the occurrence of positive ground flashes. *Journal of Geophysical Research*, *91*(D9), 9905–9909. https://doi.org/10.1029/JD091iD09p09905

Takahashi, T. (1978). Riming electrification as a charge generation mechanism in thunderstorms. *Journal of the Atmospheric Sciences*, *35*(8), 1536–1548. https://doi.org/10.1175/1520-

0469(1978)035<1536:REAACG>2.0.CO;2

Takahashi, T., & Miyawaki, K. (2002). Reexamination of riming electrification in a wind tunnel. *Journal of the Atmospheric Sciences, 59,* 1018–1025, doi:10.1175/1520-0469

Takeuti, T., Nakano, M., Brook, M., Raymond, D. J., & Krehbiel, P. (1978). The anomalous winter thunderstorms of the Hokuriku coast. *Journal of Geophysical Research*, *83*(C5), 2385–2394. https://doi.org/10.1029/JC083iC05p02385

Tessendorf, S. A., Rutledge, S. A., & Wiens, K. C. (2007a). Radar and lightning observations of normal and inverted polarity multicellular storms from STEPS. *Monthly Weather Review, 135*(11), 3682–3706. https://doi.org/10.1175/2007MWR1954.1

Tessendorf, S. A., Wiens, K. C., & Rutledge, S. A. (2007b). Radar and lightning observations of the 3 June 2000 electrically inverted storm from STEPS. *Monthly Weather Review*, 135, 3665–3681.

Weisman, M. L., & Klemp, J. B., (1982). The dependence of numerically simulated convective storms on vertical wind shear and buoyancy. *Monthly Weather Review, 110*, 504–520.

Weisman, M. L., & Klemp, J. B., (1984). The structure and classification of numerically simulated convective storms in directionally varying wind shears. *Monthly Weather Review, 112*, 2479–2498.

Weiss, S. A., Rust, W. D., MacGorman, D. R., Bruning, E. C., & Krehbiel, P. R. (2008). Evolving complex electrical structures of the STEPS 25 June 2000 multicell storm. *Monthly Weather Review, 136*(2), 741–756. https://doi.org/10.1175/2007MWR2023.1

Wiens, K. C., Rutledge, S. A., & Tessendorf, S. A. (2005). The 29 June 2000 supercell observed during STEPS. Part II: Lightning and charge structure. *Journal of the Atmospheric Sciences, 62*(12), 4151–4177. https://doi.org/10.1175/JAS3615.1

Wilks, D.S. (2011). Statistical methods in the atmospheric sciences. *International Geophysics* (3rd ed., Vol. 100). Academic Press. https://doi.org/10.1016/B978-0-12-385022-5.00026-9

Williams, E. R. (1989). The tripole structure of thunderstorms. *Journal of Geophysical Research: Atmospheres*, *94*(D11), 13151–13167. https://doi.org/10.1029/JD094iD11p13151

Williams, E. R., Lyons, W. A., Hobara, Y., Mushtak, V. C., Asencio, N., Boldi, R., et al. (2010). Ground-based detection of sprites and their parent lightning flashes over Africa during the 2006 AMMA campaign. *Quarterly Journal of the Royal Meteorological Society*, *136*: 257–271. doi:10.1002/qj.489

Williams, E. R., Mushtak, V., Rosenfeld, D., Goodman, S., & Boccippio, D. (2005). Thermodynamic conditions favorable to superlative thunderstorm updraft, mixed phase microphysics and lightning flash rate. *Atmospheric Research, 76*(2005), 288–306.

https://doi.org/10.1016/j.atmosres.2004.11.009

Williams, E. R., Zhang, R., & Rydock, J. (1991). Mixed-Phase microphysics and cloud electrification. *Journal of the Atmospheric Sciences*, *48*(19), 2195–2203.

Wilson, C. T. R. (1916). On some determinations of the sign and magnitude of electric discharges in lightning flashes. *Proceedings of the Royal Society. A.*, *92*, 555–574. https://doi.org/10.1098/rspa.1916.0040

Wilson, C. T. R. (1921). Investigations on lightning discharges and on the electric field of thunderstorms. *Philosophical Transactions of the Royal Society A: Mathematical, Physical, and Engineering Sciences*, *221*(582–593).

Young, K. C. (1993). *Microphysical Processes in Clouds*, Oxford University Press.

Ziegler, C. L., MacGorman, D. R., Ray, P. S., & Dye, J. E. (1991). A model evaluation of non-inductive graupel-ice charging in the early electrification of a mountain thunderstorm. *Journal of Geophysical Research.*, *96*, 12833–12855.